The Activity-Dependent Regulation of Protein Kinase Stability by the Localization to P-Bodies

Bo Zhang, Qian Shi, Sapna N. Varia, Siyuan Xing, Bethany M. Klett, Laura A. Cook, and Paul K. Herman[1]
Department of Molecular Genetics, The Ohio State University, Columbus, Ohio 43210

ABSTRACT The eukaryotic cytoplasm contains a variety of ribonucleoprotein (RNP) granules in addition to the better-understood membrane-bound organelles. These granules form in response to specific stress conditions and contain a number of signaling molecules important for the control of cell growth and survival. However, relatively little is known about the mechanisms responsible for, and the ultimate consequences of, this protein localization. Here, we show that the Hrr25/CK1δ protein kinase is recruited to cytoplasmic processing bodies (P-bodies) in an evolutionarily conserved manner. This recruitment requires Hrr25 kinase activity and the Dcp2 decapping enzyme, a core constituent of these RNP granules. Interestingly, the data indicate that this localization sequesters active Hrr25 away from the remainder of the cytoplasm and thereby shields this enzyme from the degradation machinery during these periods of stress. Altogether, this work illustrates how the presence within an RNP granule can alter the ultimate fate of the localized protein.

KEYWORDS ribonucleoprotein granules; processing bodies; protein kinase; protein stability; Dcp2 decapping enzyme; casein kinase 1

THE eukaryotic cell is subdivided into distinct functional areas by the presence of a variety of organelles. The best understood of these are the membrane-bound structures, like the nucleus, endoplasmic reticulum, and mitochondria. These traditional compartments are relatively stable and essential for the proper compartmentalization of the different reactions occurring in the cytoplasm. However, the cell also contains a collection of nonmembraneous organelles that are more dynamic in nature and form in response to particular cellular and environmental stimuli. Perhaps the two best characterized of these are the centrosome and nucleolus, which act as a microtubule-organizing center and a subnuclear site of ribosome assembly, respectively (Greenan *et al.* 2010; Brangwynne 2011; Brangwynne *et al.* 2011). This latter class also includes a number of recently identified cytoplasmic ribonucleoprotein (RNP) granules like the processing body (P-body) and stress granule (Anderson and Kedersha 2009; Balagopal and Parker 2009; Thomas *et al.* 2011). These cytoplasmic structures have been conserved through evolution and have been linked to a variety of human diseases, including certain neurodegenerative disorders, cancers, and autoimmune conditions (Li *et al.* 2013; Anderson *et al.* 2015). Despite this importance to human health, relatively little is known about the manner in which these RNP granules influence biological processes in the cell.

These cytoplasmic RNP granules typically assemble in response to environmental stress or particular developmental cues (Thomas *et al.* 2011). Granule formation occurs as a consequence of the regulated coalescence of specific sets of proteins and translationally repressed mRNAs at discrete sites in the cytoplasm (Anderson and Kedersha 2009; Balagopal and Parker 2009). The presence of these core proteins often depends upon specific RNA-binding motifs and/or prion-like self-assembly elements that may also have roles in the final aggregation necessary for granule formation (Gilks *et al.* 2004; Decker *et al.* 2007; Pilkington and Parker 2008; Reijns *et al.* 2008; Jonas and Izaurralde 2013). This coalescence is thought to lead to a phase transition that produces granules in a gel-like or condensed liquid phase, with contents present at concentrations higher than that in the surrounding environment (Brangwynne *et al.* 2009; Kato *et al.* 2012; Weber and Brangwynne 2012; Hyman *et al.* 2014). P-bodies, in particular, contain proteins involved in messenger RNA (mRNA) decay including the exonuclease Xrn1, the major decapping enzyme Dcp1/Dcp2, and decapping enhancers like Edc3 and Pat1 (Bashkirov *et al.* 1997; Ingelfinger *et al.* 2002; Eystathioy *et al.* 2003; Sheth and Parker 2003; Cougot *et al.* 2004; Eulalio

doi: 10.1534/genetics.116.187419
Manuscript received January 22, 2016; accepted for publication May 2, 2016; published Early Online May 3, 2016.
Supplemental material is available online at www.genetics.org/lookup/suppl/doi:10.1534/genetics.116.187419/-/DC1.
[1]Corresponding author: Department of Molecular Genetics, The Ohio State University, 484 W. 12th Ave., Rm. 105, Columbus, OH 43210. E-mail: herman.81@osu.edu

et al. 2007a; Parker and Sheth 2007). As a result, P-bodies were originally proposed to be cytoplasmic sites of mRNA decay (Sheth and Parker 2003; Franks and Lykke-Andersen 2008). However, subsequent work has demonstrated that mRNA turnover occurs normally in cells lacking P-body foci and thus the biological functions of these granules remain unclear (Stoecklin *et al.* 2006; Decker *et al.* 2007; Eulalio *et al.* 2007b; Ramachandran *et al.* 2011). More recent studies have suggested that the activities of P-bodies, and other RNP granules, may be determined by the presence of the more peripheral proteins associated with these structures. For example, these cytoplasmic granules have been found to influence cell physiology by recruiting signaling molecules important for the normal regulation of growth and survival (Arimoto *et al.* 2008; Takahara and Maeda 2012; Kedersha *et al.* 2013; Thedieck *et al.* 2013; Wippich *et al.* 2013; Shah *et al.* 2014). The reasons for this recruitment are likely manifold and similar to those that apply to the membrane-bound compartments in the cytoplasm. These include the recruited protein being responsible for a specific activity within the granule, being sequestered away from its normal site of action (and thus down-regulated), and being stored or protected within the RNP structure. As a result, it is essential that we identify the proteins localized to these RNP structures, the underlying machinery governing this recruitment, and the physiological consequences of this protein localization.

To begin to answer these questions, we undertook an examination of a representative constituent of P-body foci, the Hrr25/CK1δ protein kinase. Hrr25 belongs to the casein kinase 1 (CK1) family of protein kinases and is the yeast ortholog of the mammalian CK1δ enzyme (DeMaggio *et al.* 1992). The Hrr25/CK1δ proteins have conserved roles in ribosome maturation, vesicle trafficking, DNA repair, and chromosome segregation during meiosis (Hoekstra *et al.* 1991; Petronczki *et al.* 2006; Schafer *et al.* 2006; Ray *et al.* 2008; Grozav *et al.* 2009; Biswas *et al.* 2011; Isoda *et al.* 2011; Lord *et al.* 2011). We report here that this critical regulator of cell proliferation is efficiently recruited to P-bodies in both yeast and mammalian cells under all conditions examined. This localization depends upon a specific interaction with Dcp2, the catalytic subunit of the primary decapping enzyme in eukaryotes and a conserved core component of these RNP granules. This recruitment also requires Hrr25 kinase activity, suggesting that only the active enzyme can be localized to P-body foci. Finally, experiments with targeting-deficient variants of Hrr25 indicate that a failure to associate with P-bodies results in the rapid degradation of this kinase in stressed cells. Therefore, the P-body appears to provide a type of safe haven that can offer protection from the cytoplasmic degradation machinery during periods of duress.

Materials and Methods

Yeast growth conditions and strain construction

Standard *Escherichia coli* and yeast media and growth conditions were used throughout this study. Synthetic complete medium with 2% glucose, referred to as SC-dextrose (SCD), was used for yeast culture unless otherwise noted. The glucose starvation medium was SCD without the added glucose and was referred to as SC. Expression from the *CUP1* promoter was induced by the addition of 100 μM $CuSO_4$ to the growth medium. For the indicated stress treatments, yeast strains were grown to midlog phase in SCD medium and then transferred for 20 min to SC medium lacking glucose (−Glc), H_2O, SC containing 2% galactose (SCGal), or SCD medium containing 3 mM H_2O_2, 0.5% NaN_3, or 0.4% HCl.

To reduce Hrr25 protein levels in cells, we used a previously described strain, KKY387, that expresses an unstable, degron-tagged version of Hrr25 ($Hrr25^{degron}$) under the control of a galactose-inducible promoter (Kafadar *et al.* 2003; Ray *et al.* 2008). Briefly, this strain was grown to midlog phase in SCGal medium and then transferred to SCD for 8 hr to repress $Hrr25^{degron}$ expression and arrest growth. These growth-arrested cells were then transferred to SC medium lacking glucose and P-body formation was assessed by fluorescence microscopy. Cells carrying the wild-type *HRR25* locus were subjected to the same experimental regimen and served as the +Hrr25 control for these experiments.

The yeast strains used are listed in Supplemental Material, Table S1, Table S2, and File S1. Tandem affinity purification (TAP) or mCherry-tagged yeast strains were generated with a previously described PCR-based strategy using a TAP (pPHY4174) or mCh (pPHY3932) plasmid, respectively (Longtine *et al.* 1998). To construct strains with chromosomally encoded mutant alleles of *HRR25*, we first introduced a single-copy *URA3* plasmid carrying a *HRR25-mCh* construct (pPHY3741) into the wild-type BY4741 strain. Second, the same PCR-based deletion method was used to replace the chromosomal *HRR25* locus with the *LEU2* gene (Longtine *et al.* 1998). Third, mEGFP-tagged versions of different *hrr25* alleles were introduced on the integrating plasmid, pRS403, and targeted to the *HRR25* locus. This plasmid contains the *HIS3* gene and successful integration was indicated by the selection for growth on media lacking histidine. These strains were subsequently plated onto SCD plates containing 0.8 mg/ml 5-fluoroorotic acid (5-FOA; US Biological) to counterselect against the *URA3* plasmid carrying the wild-type *HRR25* locus. Finally, cells were examined by fluorescence microscopy and those with an mEGFP signal, but no mCh fluorescence, were saved. The presence of the *hrr25* mutations in each strain were further confirmed by a PCR analysis using the appropriate mutation-specific primers.

Mammalian cell culture and transfection

Cell culture and transfection were performed as described (Majumder and Fisk 2013; Varia *et al.* 2013). Briefly, HeLa S3 cells were grown in Dulbecco's modified Eagle's medium (DMEM) supplemented with 10% fetal bovine serum and 1% penicillin/streptomycin antibiotic. The RFP-*RCK1* construct (a gift from Daniel Schoenberg) was transfected into the cells using FuGENE (Promega, Madison, WI) as per the manufacturer's instructions. The cells were incubated at 37° with 5% CO_2.

Plasmid construction

The plasmids used in this study are listed in Table S3. The *PAT1-mCh* (pPHY3785, *CEN*, *URA3*) and *PAT1-GFP* (pPHY3648, *CEN*, *URA3*) plasmids were described previously (Ramachandran *et al.* 2011; Shah *et al.* 2014). The *DCP2-RFP* (pPHY3714, *CEN*, *LEU2*), *DHH1-GFP* (pPHY2659, *CEN*, *URA3*), *LSM1-mCh* (pPHY3698, *CEN*, *LEU2*) and *EDC3-mCh* (pPHY3660 *CEN*, *URA3*) plasmids were provided by Claudio de Virgilio, Tien-Hsien Chang, Anita Hopper, and Roy Parker, respectively (Beckham *et al.* 2007; Buchan *et al.* 2011). Plasmids used for PCR-based deletion or tagging of specific loci were derived from the pFA6a series; these constructs had *LEU2* replacing *KANMX6* and either mCh or the TAP tag replacing GFP (Longtine *et al.* 1998). To construct the *HRR25* plasmids used in this study, *HRR25* fragments were generated with a PCR reaction using genomic DNA as template and then inserted into vectors containing the *HRR25* promoter, an appropriate in-frame tag, such as GFP, mCherry, or 3× HA, and finally the *ADH1* terminator. The *HRR25* promoter was replaced by the promoter from the *CUP1* or *GPD* genes, where needed. Mutagenesis was performed with the GeneArt site-directed mutagenesis system (Life Technologies) or by a gap-repair strategy where the mutations were incorporated into a particular PCR primer.

Microscopy and data analysis

Cells expressing the indicated fusion constructs were grown to early log phase (0.6–0.8 OD_{600} units/ml) before exposure to the indicated stress or drug treatment. The cells were then collected by centrifugation and spotted onto a microscope slide. The time between the start of each treatment and image capture was 20–30 min unless otherwise noted. Two microscope systems were used to collect the images presented here. Most images were taken with a spinning disk confocal system (UltraVIEW Vox CSUX1 system; Perkin-Elmer, Norwalk, CT) with 405-, 488-, and 561-nm solid state lasers and dual back-thinned EM CCD cameras (C9100-13; Hamamatsu Photonics) using a Nikon Ti-E inverted microscope without binning, under single camera mode with ×100/1.4 N.A. Plan-Apo objective lenses (Nikon, Garden City, NY). For the initial screening of deletion strains and the disassembly analysis, an inverted microscope (Eclipse Ti; Nikon) equipped with an Andor Zyla digital camera, Nikon HC filters and a ×100/1.45 N.A. Plan-Apo objective lens (Nikon) was used.

Images were taken with the Volocity software package (Perkin-Elmer) and analyzed with ImageJ software (National Institutes of Health) as described (Wang *et al.* 2014). Images in figures were maximum-intensity projections of *z*-sections spaced at 0.25 μm except where otherwise noted. For the quantitation of the fraction of cells that contain foci, the data represent the average of two or three experiments that examined at least 100 cells in each case. To quantify P-body foci intensity, images were sum-slice projections of *z*-sections spaced at 0.45 μm. The area of each P-body focus was selected and measured with ImageJ to determine the total intensity. The background within two radii of each focus was measured and subtracted from the total to generate the final intensity of the focus. Ten representative cells (based on the distribution of foci number) were selected for analysis and the average fluorescence intensity was calculated for each time point. The data shown represent the average of three such independent measurements.

Immunofluorescence

Indirect immunofluorescence was performed as described (Kedersha and Anderson 2007; Varia *et al.* 2013). Briefly, the cells were grown on glass coverslips in a six-well dish and harvested at 50–60% confluency. Cells were washed with phosphate-buffered saline (PBS) and fixed with 4% paraformaldehyde in PBS for 15 min at room temperature. Methanol was immediately added and the cells were incubated for 10 min at −20°. The cells were rinsed three times with PBS containing 0.5% normal goat serum (blocking reagent) and then incubated with the primary antibody, rabbit anti-CK1δ (Pierce Chemical, Rockford, IL), for 1 hr at room temperature. After three washes with PBS containing normal goat serum (PBS/NGS), the cells were incubated with the secondary antibody, donkey anti-rabbit conjugated with FITC (Alexa Fluor 488; Invitrogen, Carlsbad, CA). DAPI was added to the final PBS wash in order to label DNA.

Western immunoblotting and co-immunoprecipitation

Protein samples for Western blotting were prepared with a glass bead lysis method, separated on 7.5% SDS-polyacrylamide gels, and transferred to nitrocellulose membranes (GE Healthcare) as described (Budovskaya *et al.* 2002, 2004). The membranes were then probed with the appropriate primary and secondary antibodies. The Supersignal chemiluminescent substrate (Pierce Chemical) was subsequently used to detect the reactive bands. Extracts for co-immunoprecipitation were prepared by resuspending cells in lysis buffer [25 mM Tris-HCl (pH 7.4), 140 mM NaCl, 1% Tween-20, 1 mM PMSF] and agitating with glass beads. TAP- or HA-tagged proteins were immunoprecipitated with sheep anti-mouse IgG magnetic Dynabeads (Invitrogen) or anti-HA Sepharose (Roche). Protease and phosphatase inhibitors were present at all steps. The extent of interaction was then assessed by Western blotting with the anti-GFP antibody (Roche).

Examining the rate of Hrr25 protein degradation

lmmunoprecipitations from yeast cells labeled with Tran^{35}S-label (MP Biomedicals) were performed as described previously (Herman and Emr 1990; Simon and Kornitzer 2014). Briefly, expression from a *CUP1pro-HRR25-HA* construct was induced by the addition of 100 μM $CuSO_4$ for 15 min at 30°. At this time, 50 OD_{600} units of cells were collected by centrifugation and placed in a medium containing the Tran^{35}S-label mix at a final concentration of 20 μCi/OD_{600} for 15 min at 30°. This labeling reaction was terminated by the addition of a chase solution that resulted in final methionine and cysteine concentrations of 5 mM and 1 mM, respectively.

The cells were then divided into five aliquots, washed, and moved to SC media containing chase solution but without glucose for the starvation. Samples were collected at the indicated time points and immunoprecipitation was performed as described above. The precipitated radiolabeled proteins were separated by electrophoresis on 7.5% SDS-polyacrylamide gels. Following electrophoresis, the gels were fixed and dried before autoradiography. The relative radioactivity present was quantified with the ImageJ software package.

Data availability

The authors state that all data necessary for confirming the conclusions presented in the article are represented fully within the article.

Results

The localization of Hrr25/CK1δ to P-bodies is an evolutionarily conserved phenomenon

We have previously shown that Hrr25 is present specifically in P-body foci in stationary phase cells (Shah *et al.* 2014). However, these cytoplasmic granules are induced by a variety of different stress conditions and we tested here whether this protein kinase was associated with P-body foci at these times. For this analysis, we used a yeast strain expressing an mEGFP-tagged Hrr25 protein and an mCherry-tagged Edc3 (Edc3-mCh) reporter that served as the marker for P-body foci. Both fusion constructs were integrated into the genome and expressed from their respective endogenous promoters. For each condition, we found that Hrr25 was associated with P-body foci and that the colocalization between Hrr25 and Edc3 was >90% (Figure 1A; Figure S1A). This level of colocalization was equivalent or higher than that observed between any pair of P-body reporters (Mitchell *et al.* 2013; Shah *et al.* 2014). This observation was not restricted to Edc3, as Hrr25 exhibited a similar degree of colocalization with other P-body constituents, including Dcp2, Pat1, and Lsm1 (Figure 1B). Consistent with this localization, Hrr25 was detected in immunoprecipitates with several different P-body proteins (Figure 1C; Figure S1B). Previous larger-scale studies had identified potential interactions between Hrr25 and particular P-body constituents (Ito *et al.* 2001; Ho *et al.* 2002; Cary *et al.* 2015). Moreover, we found that the mammalian ortholog of Hrr25, CK1δ, was also found in P-body foci (Figure 1D). For this experiment, P-bodies were induced by the overexpression of RCK1, the mammalian ortholog of the yeast Dhh1 RNA helicase (Cougot *et al.* 2004). Both Dhh1 and RCK1 have been shown to be associated with P-body foci (Sheth and Parker 2003; Cougot *et al.* 2004). Finally, the presence of Hrr25 in foci was found to be dependent upon P-body formation as very few Hrr25 puncta were detected in cells defective for the assembly of these cytoplasmic granules (Figure 1E; Figure S1, C–F). Altogether, these data indicated that Hrr25 was a constant constituent of P-bodies in yeast cells and that this recruitment to P-body foci has been evolutionarily conserved from yeast to humans.

Hrr25 is not required for P-body formation and disassembly

To test whether Hrr25 has a role in P-body assembly, we examined the consequences of altering either Hrr25 protein or activity levels in cells. Since this protein kinase is required for viability (Figure S2A), we took advantage of a yeast strain that expresses an unstable, degron-tagged version of this enzyme (Giaever *et al.* 2002; Kafadar *et al.* 2003). This variant, $Hrr25^{degron}$, was expressed from an inducible *GAL* promoter that is strongly repressed by the presence of glucose. A shift to a glucose-containing medium therefore results in a growth arrest due to the shutdown of Hrr25 production and the rapid turnover of the preexisting pool of this protein kinase (Kafadar *et al.* 2003). Following this arrest, the cells were transferred to a medium lacking glucose to induce P-body formation. Using this regimen, we found that P-bodies were produced at a similar level in the arrested cells, suggesting that Hrr25 was not needed for efficient P-body assembly (Figure S2B). To confirm this result, we also examined P-body formation in a strain that expressed a kinase-defective variant of Hrr25 ($Hrr25^{KD}$) where lysine-38 in the catalytic site is replaced with an alanine residue (Murakami *et al.* 1999). Cells that express only this version of Hrr25 are viable but exhibit a significant growth defect (Figure S2A). Consistent with the above results, we found that P-body assembly (and disassembly) was not affected by the diminished levels of Hrr25 activity in this strain (Figure 2, A and B; Figure S2C). Finally, we found that the overexpression of Hrr25 did not have a significant effect on P-body numbers in either stressed or nonstressed cells (Figure S2D). In all, these results indicated that neither Hrr25 nor its kinase activity was needed for efficient P-body assembly.

The kinase activity of Hrr25 is required for its efficient localization to P-bodies

In contrast to the above results, we found that Hrr25 kinase activity was required for its own recruitment to P-bodies. For example, the kinase-defective variant, $Hrr25^{KD}$, was not recruited to P-body foci upon glucose deprivation (Figure 2C). These results were confirmed by studies with a strain expressing a conditional allele of *HRR25* that renders the encoded protein sensitive to the ATP analog, 1-NM PP1 (Bishop *et al.* 2001; Petronczki *et al.* 2006). This protein, $Hrr25^{AS}$, has a glycine residue replacing the isoleucine at position 82 (I82G) and is referred to as an analog-sensitive version of this protein kinase (Bishop *et al.* 2001; Petronczki *et al.* 2006). Here, we found that an exposure to this drug resulted in a significant defect in $Hrr25^{AS}$ localization to P-bodies (Figure 2D; Figure S2, E and F). This result suggested that the above observations with the constitutively inactive variant of Hrr25 were not due to secondary consequences associated with the long-term loss of Hrr25 activity. We also found that Hrr25 kinase activity was needed for the continued presence of this protein in P-body foci. Specifically, the addition of 1-NM PP1 to cells that already contained P-bodies resulted in the rapid return of the foci-associated $Hrr25^{AS}$

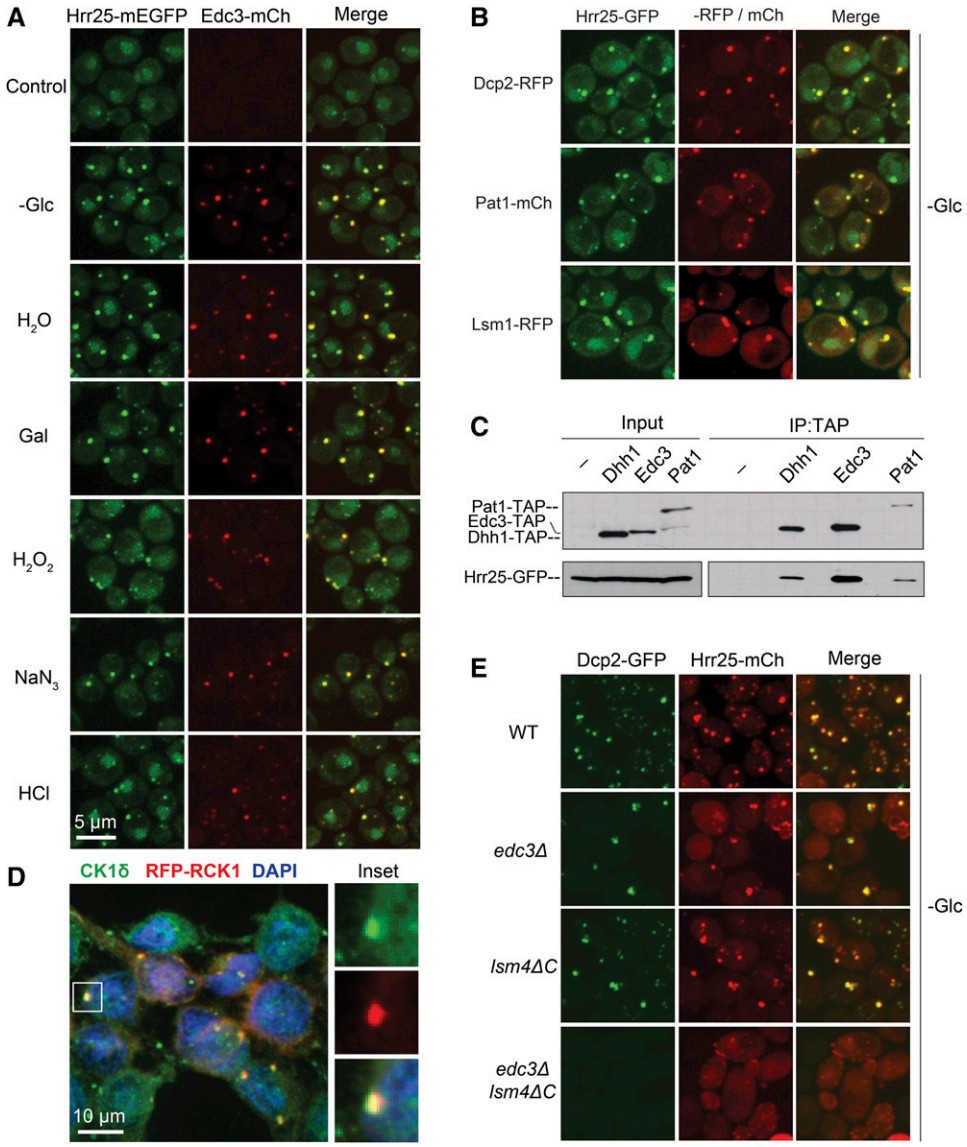

Figure 1 The localization of the Hrr25/CK1δ protein kinase to P-bodies is an evolutionarily conserved phenomenon. (A) Hrr25 was efficiently recruited to P-bodies in all stress conditions examined. Cells expressing Hrr25-mEGFP and Edc3-mCh were grown to midlog phase and then subjected to the indicated stress conditions. Focus formation was then assessed by confocal microscopy. (B) Hrr25 exhibited a significant level of colocalization with multiple P-body reporters. Strains expressing Hrr25-mEGFP and the indicated P-body reporters were grown to midlog phase and then transferred to a medium lacking glucose to induce P-body formation. (C) Hrr25 was detected in immunoprecipitates with multiple P-body proteins. The indicated TAP-tagged P-body proteins were precipitated from yeast cell extracts and the relative level of the associated Hrr25-GFP protein was assessed by Western blotting. (D) Human CK1δ was associated with P-bodies. P-body formation was induced in HeLa cells by the overexpression of an RCK1-RFP construct and an antibody to the CK1δ enzyme was used for immunofluorescence. RCK1 is the mammalian ortholog of the yeast Dhh1 RNA helicase (Sheth and Parker 2003; Cougot *et al.* 2004). The panels at the right show the CK1δ, RFP-RCK1, and merged images for the indicated focus in the main panel. (E) Hrr25 foci were absent from cells defective for P-body assembly. The localization of Dcp2-GFP and Hrr25-mCh was determined by confocal microscopy after the indicated strains had been transferred to a medium lacking glucose for 20 min. Quantitation of these data and the +Glc control images are shown in Figure S1, C and D, respectively. P-body assembly has been shown to be compromised in both the *edc3*Δ *lsm4*Δ*C* and *pat1*Δ mutants (Sheth and Parker 2003; Decker *et al.* 2007; Ramachandran *et al.* 2011).

back to the cytosol (Figure 2E). Collectively, these results indicated that Hrr25 kinase activity was necessary for its localization to P-bodies.

Hrr25 recruitment to P-bodies requires the presence of Dcp2, the catalytic subunit of the decapping enzyme

Hrr25 could be recruited to P-bodies as a result of an interaction with either a protein or mRNA component of these structures. However, Hrr25 does not possess any known RNA-binding motif and no RNA-binding activity has been demonstrated for this protein. Therefore, we tested whether Hrr25 localization to P-bodies was dependent upon any of the known protein constituents of these granules. For this analysis, we examined 43 yeast deletion strains, each lacking a particular P-body protein (Table S1) (Mitchell *et al.* 2013). These studies identified only one candidate, the *dcp2*Δ mutant, that lacks the catalytic subunit of the decapping enzyme. Dcp2 was one of the first proteins identified in P-body foci and is generally thought of as a core constituent of these granules (van Dijk *et al.* 2002; Sheth and Parker 2003; Cougot *et al.* 2004). The *dcp2*Δ strain exhibited a severe defect in Hrr25 localization, as there were almost no visible Hrr25 foci following glucose deprivation (Figure 3, A and B; Figure S3A). A similar defect was observed under all other stress conditions examined, indicating that the presence of Dcp2 was generally required for Hrr25 localization to P-bodies (Figure 3, A and B).

Since Dcp2 is part of the decapping enzyme, the failure of Hrr25 to associate with P-body foci in *dcp2*Δ mutants could be due to the decreased levels of uncapped mRNA in this strain. However, two results suggested that the defect was more likely due to the absence of the Dcp2 protein proper. First, we found that Hrr25 was efficiently localized to P-bodies in a *dcp1*Δ strain (Figure 3C). This mutant lacks Dcp1, the regulatory

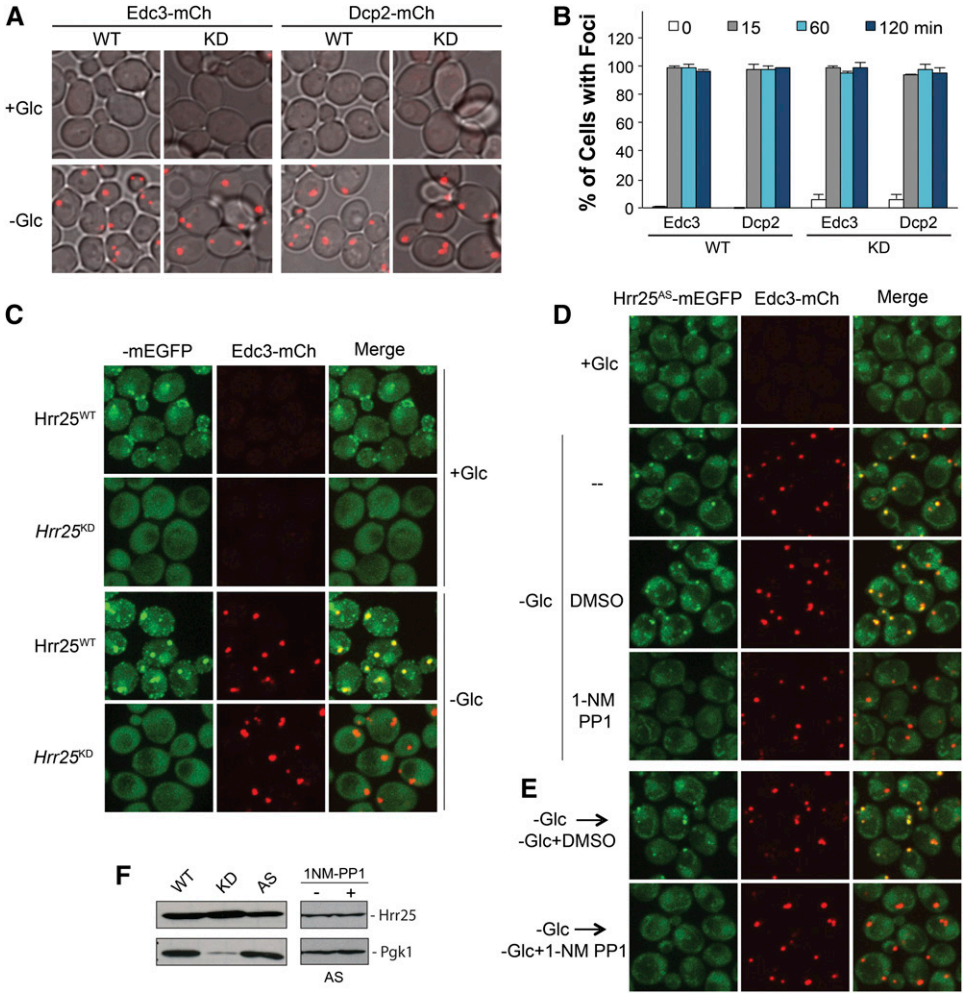

Figure 2 Hrr25 kinase activity was required for its recruitment to P-body foci. (A and B) P-body assembly did not require Hrr25 kinase activity. Strains expressing either the wild-type (WT) or a kinase-defective (KD) Hrr25 enzyme were grown to midlog phase and then transferred to a medium lacking glucose for the indicated times. P-body formation was then assessed by confocal microscopy at the indicated times (B); images at the 60-min time point are shown in A. The Hrr25^{KD} protein has an alanine replacing the critical lysine-38 residue in the catalytic site (Murakami *et al.* 1999). (C) A kinase-defective variant of Hrr25 did not localize to P-body foci. Strains expressing either the WT or a KD Hrr25 enzyme were grown to midlog phase and then transferred to a medium lacking glucose to induce P-body formation. (D) Hrr25 kinase activity was required for P-body localization. Cells expressing an analog-sensitive version of Hrr25, Hrr25^{AS}, were transferred to a medium lacking glucose with or without the drug, 1-NM PP1, for 45 min. P-body foci formation was then assessed by confocal microscopy. (E) The inhibition of Hrr25 kinase activity resulted in the rapid loss of Hrr25 from P-body foci. Cells expressing the Hrr25^{AS} protein were starved for glucose to induce P-body formation and then treated with the drug, 1-NM PP1, for 15 min to inhibit Hrr25 activity. The localization of Hrr25^{AS}-mEGFP and Edc3-mCh were then assessed by confocal microscopy. (F) Western blot analysis of the levels of WT, KD, and AS versions of Hrr25 in midlog phase cultures of each strain. The low level of Pgk1 in the *hrr25-kd* mutant is most likely a consequence of the significant growth defect associated with this strain. The right hand blots show that the levels of the Hrr25^{AS} protein were similar after 45 min of glucose starvation in the presence or absence of the 1-NM PP1 inhibitor.

subunit of the Dcp1/Dcp2 decapping complex, and therefore possesses diminished levels of decapping activity (Beelman *et al.* 1996; van Dijk *et al.* 2002; She *et al.* 2006). The second observation was that Hrr25 was detected in Dcp2 immunoprecipitates specifically in cells that had been deprived of glucose and thus contained P-body foci (Figure 3D). Very little, if any, Hrr25 was associated with Dcp2 in log-phase cells where P-body numbers are very low. In addition, this interaction required Hrr25 kinase activity, as less Hrr25^{AS} protein was associated with Dcp2 after an exposure to the drug, 1-NM PP1 (Figure 3E). These data are therefore consistent with a model where Dcp2 interacts, either directly or indirectly, with Hrr25 and thereby recruits this protein kinase to P-body foci. Additional support for this model was provided by an analysis of two mutants, *xrn1*Δ and *sbp1*Δ, that form P-body-related structures in log-phase cells (Sheth and Parker 2003; Segal *et al.* 2006). The key point here is that these log-phase foci or aggregates differ with respect to the amount of associated Dcp2. In particular, whereas Dcp2 was readily apparent in the *xrn1*Δ foci, it was either absent or present at very low levels in the log-phase foci in *sbp1*Δ cells (Figure S3B). Correspondingly, Hrr25-GFP fluorescence was detectable only in the log-phase *xrn1*Δ foci (albeit at a low level). Finally, we also detected Hrr25 in the P-body foci that are found in log-phase cells of the *dcp1*Δ mutant (Figure S3C) (Teixeira and Parker 2007). These latter foci also contain the Dcp2 protein. Altogether, the data here suggest that Hrr25 was recruited to P-body foci as a result of an interaction with the Dcp2 protein.

Hrr25 recruitment to foci occurs after that of the core constituents

The above results suggested that Hrr25 might be a more peripheral component of the P-body granule. To examine this possibility further, we assessed the timing of Hrr25 recruitment relative to that of the core constituents, Edc3 and Dcp2. For this analysis, the relative intensity of the foci-associated fluorescence was assessed at different times up to 120 min after transfer to a medium lacking glucose. A Western blot analysis indicated that the levels of Hrr25 did not change appreciably during this time period (Figure 4A). In general, we found that cells contained multiple

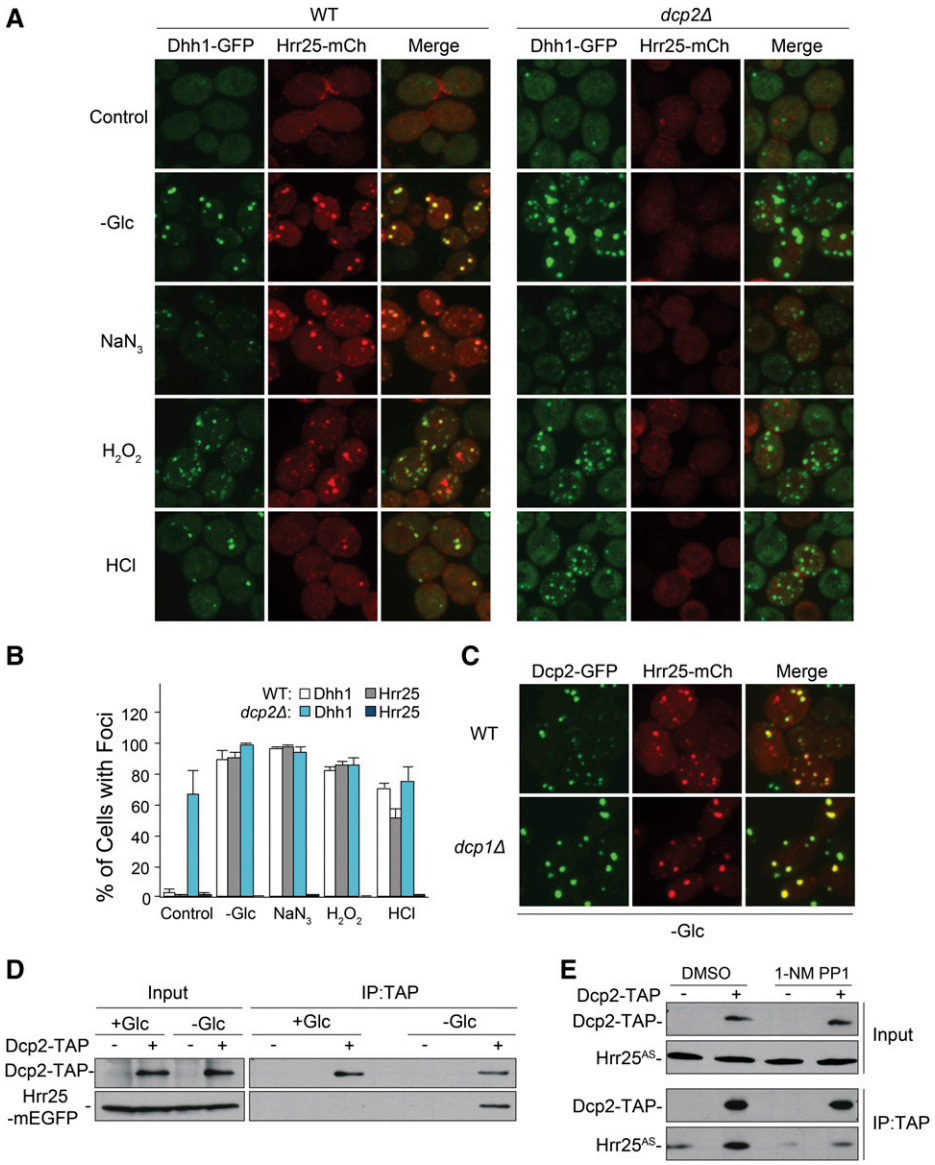

Figure 3 The recruitment of Hrr25 to P-bodies required Dcp2, the catalytic subunit of the decapping enzyme. (A and B) The presence of Dcp2 was generally required for Hrr25 localization to P-bodies. P-bodies were induced by the indicated stress conditions in either wild-type or *dcp2*Δ cells. P-body foci were visualized by confocal microscopy (A) and the fraction of cells with foci were quantified (in B). (C) Hrr25 localization to P-bodies did not require Dcp1. Hrr25-mCh localization was assessed by confocal microscopy after glucose deprivation of wild-type or *dcp1*Δ cells. (D) Hrr25 was associated with Dcp2 specifically in glucose-deprived cells. TAP-tagged Dcp2 was precipitated from extracts prepared from either midlog phase cells (+*Glc*) or cells that had been starved for glucose for 30 min (−*Glc*). The amount of coprecipitating Hrr25-mEGFP was assessed by Western blotting with an antibody to GFP. (E) The inhibition of Hrr25 kinase activity disrupted the Hrr25-Dcp2 interaction. TAP-tagged Dcp2 was precipitated from glucose-starved cells expressing the $Hrr25^{AS}$ protein in the presence or absence of the drug, 1-NM PP1. The relative levels of the associated $Hrr25^{AS}$ protein were subsequently assessed by Western blotting.

smaller foci after 10–15 min of glucose deprivation and that these foci appeared to coalesce into a smaller number of larger structures at later times (Figure 4B; Figure S4A). The maximum level of fluorescence was generally achieved within 120 min and the value at this time was set as the 100% level for our analysis. Using this approach, we found that Hrr25 reached its maximum fluorescence at a rate that was slower than that for both Edc3 and Dcp2 (Figure 4, B and C; Figure S4, A and B). This recruitment to P-bodies was accompanied by a loss of Hrr25 at the spindle pole body and bud neck, two structures that Hrr25 is known to associate with in log-phase cells (Figure 4D) (Kafadar *et al.* 2003; Lusk *et al.* 2007). An analogous result was observed with a time-course analysis of P-body disassembly. In this case, the decrease in foci-associated fluorescence was assessed after the readdition of a glucose-containing medium. The glucose concentration used was 0.2% instead of the standard 2%, in order to slow down the disassembly process and facilitate the detection of any potential differences (Figure S4C). We found that Hrr25 foci number decreased at a faster rate than that observed for either Edc3 or Dcp2, suggesting that Hrr25 left the granule before these two core constituents (Figure 4, E and F; Figure S4, D and E). These timing experiments are therefore consistent with the above data, indicating that Dcp2 was required for Hrr25 localization to these RNP granules.

Two sequence elements in the central domain of Hrr25 are required for P-body localization

A structure–function analysis of Hrr25 was carried out to determine the domains required for the localization to P-bodies. This protein contains three recognizable domains: the protein kinase domain (residues 1–293); a central region of unknown function (294–394); and a C-terminal domain that is rich in proline and glutamine residues (P/Q rich, 395–494) (Figure 5A) (Petronczki *et al.* 2006). To determine which of these was important for P-body localization, we generated GFP-tagged versions of the Hrr25 truncations shown in Figure 5B. The

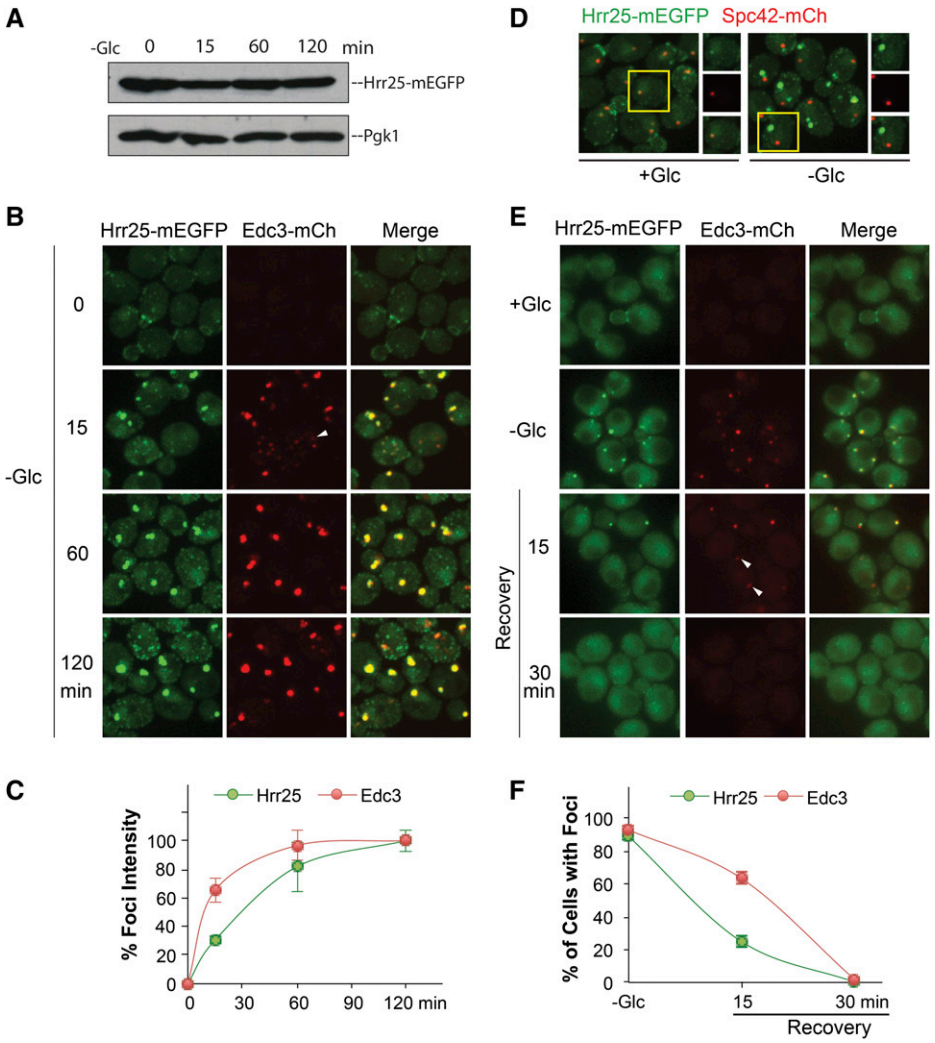

Figure 4 The kinetics of Hrr25 recruitment to P-body foci. (A) Hrr25 protein levels were constant for the entire 120-min incubation period. Midlog phase cells were transferred to a medium lacking glucose for the indicated times and the levels of Hrr25-mEGFP were assessed by Western blotting. (B and C) Hrr25 was recruited to P-body foci with slower kinetics than Edc3. Cells expressing Hrr25-mEGFP and Edc3-mCh were transferred to a medium lacking glucose and visualized by confocal microscopy at the indicated times. The graph in C indicates the average fluorescence intensities of foci at the indicated times. (D) Hrr25 was not associated with the spindle pole body (SPB) following glucose deprivation. Cells expressing Hrr25-mEGFP and Spc42-mCh were analyzed by confocal microscopy in midlog phase (+Glc) or after transfer to a medium lacking glucose (−Glc). Hrr25 colocalized with the SPB marker, Spc42-mCh, in dividing cells but not in the glucose-starved cells where P-bodies were forming. (E and F) The loss of Hrr25 foci was more rapid than that observed for Edc3 following glucose readdition. Cells expressing Hrr25-mEGFP and Edc3-mCh were transferred from a medium lacking glucose to SC minimal containing 0.2% glucose to induce P-body disassembly (Recovery). Cells were visualized by fluorescence microscopy at the indicated times (E) and the percentage of cells with foci were quantified (F). The white arrowheads indicate Edc3-containing foci with little, if any, Hrr25-associated fluorescence.

analysis of these constructs suggested that both the kinase and central domains were required for P-body association (Figure 5B). However, neither of these domains when expressed alone was sufficient for this targeting. The fact that the C-terminal P/Q-rich domain was dispensable for P-body localization was somewhat surprising, as this region is predicted to be intrinsically disordered and to have the potential to form prion-like structures (Michelitsch and Weissman 2000). These types of domains are present in a number of RNP granule constituents and have been shown to be important in several cases for the localization to, and even assembly of, these granules (Jonas and Izaurralde 2013).

A more-detailed truncation analysis identified two sequence elements in the central domain that were critical for Hrr25 localization to P-bodies (Figure 5A; Figure S5A). These motifs were designated P-body localization **s**ignals, PLS1 and PLS2. To examine the importance of particular amino acids in these elements, a series of alterations were constructed that changed two or more biochemically similar residues to alanines (Figure S5B). These experiments identified two positively charged residues in PLS1 (R294 and K297) and two phenylalanines in PLS2 (F344 and F348) as critical for P-body localization. Changing these residues in either localization element alone resulted in a significant defect in Hrr25 recruitment to P-bodies; these variants were designated PLS1* and PLS2*, respectively (Figure 5, A and C; Figure S5C). These alterations also disrupted the Hrr25 interaction with Dcp2 that was detected in co-immunoprecipitation assays (Figure 5D). Therefore, both PLS1 and PLS2 appear to be necessary for the proper localization of Hrr25 to P-body foci. It is important to note that these alterations in PLS1 and PLS2 did not have a significant effect on cell growth or the number of P-body foci (Figure 5E; Figure S5E). These results therefore suggested that the localization defects associated with PLS1* or PLS2* were not due to effects on Hrr25 kinase activity. Instead, these studies identified Hrr25 alterations that disrupt P-body localization without having a significant effect on the essential mitotic activities of this protein.

The recruitment to P-bodies protected the active Hrr25 enzyme from degradation

To assess the biological significance of Hrr25 recruitment to P-bodies, we examined the fate of this protein in the *dcp2*Δ

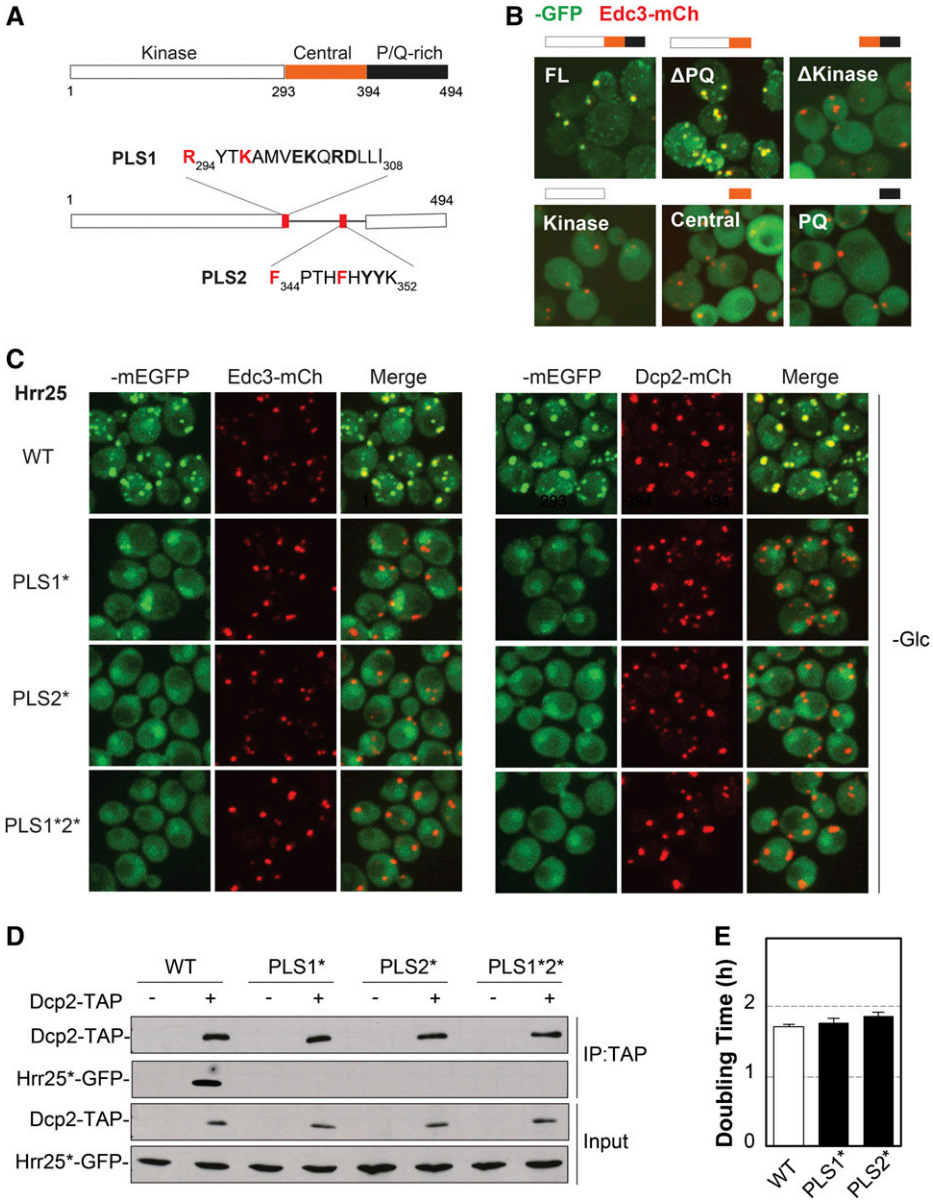

Figure 5 Two distinct sequence elements in the central domain of Hrr25 were necessary for P-body localization. (A) The domain structure of Hrr25 (top) and the location and sequence of the PLS1 and PLS2 localization signals (bottom). The two residues altered in the PLS1* and PLS* variants are indicated in red. (B) The kinase and central domains of Hrr25 were required for P-body localization. Wild-type cells were transformed with plasmids expressing the indicated GFP-tagged Hrr25 truncation constructs. The localization of these fusion proteins was assessed by fluorescence microscopy after glucose starvation. FL, full-length Hrr25. (C) Alterations in either PLS1 or PLS2 resulted in a loss of Hrr25 localization to P-bodies. Cells expressing the indicated mEGFP-tagged Hrr25 proteins were grown to midlog phase, transferred to a medium lacking glucose, and then visualized by confocal microscopy. (D) Both the PLS1 and PLS2 elements were required for the Hrr25 interaction with Dcp2. TAP-tagged Dcp2 was precipitated from cell extracts and the relative levels of the associated Hrr25 proteins were assessed by Western blotting. (E) Alterations in PLS1 or PLS2 that disrupted P-body localization (PLS1* and PLS2*) did not have a significant effect on the mitotic growth rate. The doubling times shown in the graph are the averages obtained from three independent growth curve determinations.

mutant that lacks the likely targeting subunit for this protein kinase. For this experiment, wild-type and *dcp2*Δ cells were transferred to a medium lacking glucose for up to 24 hr and Hrr25 levels were assessed by Western blotting at the indicated times. We found that the Hrr25 protein was unstable in the *dcp2*Δ mutant and that most of this protein was degraded within 2 hr of glucose starvation (Figure 6A). In contrast, the levels of Hrr25 remained relatively constant over the entire 24-hr starvation period in the wild-type control. It is unlikely that the higher Hrr25 levels in the wild-type strain are due to new synthesis as protein translation rates decrease by >90% following glucose deprivation (Ashe *et al.* 2000). To ensure that this instability was due to the loss of P-body localization and not some other consequence associated with the absence of Dcp2, we also examined strains expressing the PLS1* and PLS2* variants that are defective for P-body localization (see Figure 5A). We found that these localization-defective variants were also unstable relative to the wild-type protein in glucose-starved cells (Figure 6B). These studies therefore suggested that a failure to localize to P-bodies resulted in a more rapid turnover of the Hrr25 protein. To directly test this possibility, we assessed the rate of Hrr25 decay with a pulse-chase experiment performed with wild-type and *dcp2*Δ cells under glucose starvation conditions. These studies indicated that the Hrr25 protein was indeed more rapidly turned over in the *dcp2*Δ mutant (Figure S6). Moreover, we found that the turnover of the PLS1* variant was significantly slowed by the addition of an inhibitor of the proteasome complex (Figure 6C). Altogether, these data are consistent with Hrr25 being degraded in a proteasome-dependent manner when it is not sequestered within the P-body. This sequestration may therefore allow the cell to maintain a functional reserve of this enzyme. Since our previous data showed that P-bodies are required for the long-term survival of stationary phase

cells, we tested whether this survival was compromised in cells expressing only the PLS1* variant of Hrr25 (Ramachandran *et al.* 2011). However, we found no significant defect in these cells, suggesting that this sequestered pool of Hrr25 must be required for some other yet to be determined activity of the P-body. Nonetheless, the data here demonstrate how the localization within an RNP granule can influence the ultimate fate of a cytoplasmic protein.

Discussion

RNP granules, like P-bodies, are nonmembranous compartments that result from the concentration of particular mRNAs and proteins at discrete sites in the cytoplasm. Although an ever-increasing number of proteins are being found associated with these structures (Kedersha *et al.* 2013; Mitchell *et al.* 2013; Shah *et al.* 2014), relatively little is known about the mechanisms responsible for, and the ultimate consequences of, this recruitment. In this study, we found that the Hrr25/CK1δ protein kinase, an essential regulator of cell proliferation, is recruited to cytoplasmic P-bodies through a specific interaction with Dcp2, the major decapping enzyme in eukaryotes and a core constituent of these granules. This is the first detailed characterization of the mechanisms underlying the recruitment of a signaling molecule to this RNP structure. Interestingly, the data here indicate that this association serves to sequester active Hrr25 away from the remainder of the cytoplasm and thereby protects Hrr25 from the degradation machinery during these periods of stress (Figure 6D).

This localization to P-bodies was found to require Hrr25 kinase activity and two short sequence motifs in the central domain of this protein. Alterations affecting any one of these three regions resulted in a significant defect in P-body association. Although these alterations could affect granule localization indirectly, the simplest interpretation of the data is that PLS1 and PLS2 are P-body targeting determinants. Based on a recent crystal structure, both PLS1 and PLS2 are located within a well-ordered alpha-helical domain that is packed against the C-terminal lobe of the Hrr25 protein kinase domain (K. Corbett, personal communication). The residues that make up PLS1 (294–308) are solvent exposed and could directly contact Dcp2 and thereby recruit Hrr25 to P-body foci. The requirement for kinase activity is also significant, as it suggests that the Hrr25 protein in P-bodies could be active. Moreover, this observation argues against the possibility that it is only misfolded, nonfunctional forms of Hrr25 that are being recruited to these foci. Instead, these data are consistent with a Hrr25-catalyzed phosphorylation being critical for the P-body localization of this protein kinase. Identifying the target of this activity will be important for a full understanding of the mechanisms governing Hrr25 recruitment to these RNP granules.

The key question that remains is what are the physiological consequences of this protein localization? The data here indicate that the presence of Hrr25 in P-bodies may serve to maintain the levels of this enzyme by limiting its turnover in

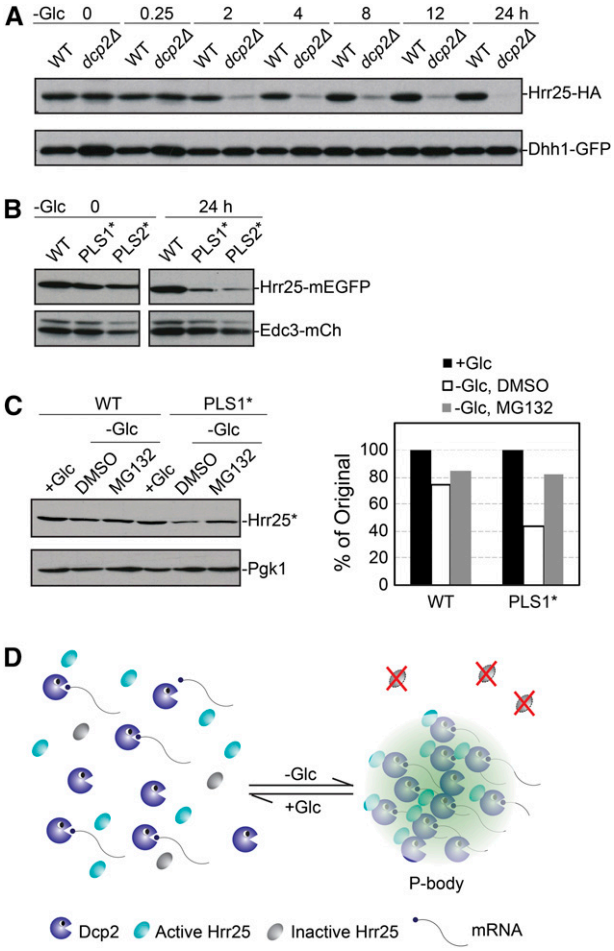

Figure 6 A failure to localize to P-bodies resulted in the rapid turnover of Hrr25. (A) Hrr25 protein levels significantly decreased in *dcp2*Δ cells upon glucose starvation. WT and *dcp2*Δ cells were starved for glucose for the indicated times and the levels of Hrr25 were then assessed by Western blotting. (B) Alterations of the PLS1 or PLS2 motifs resulted in the destabilization of Hrr25 upon glucose starvation. Strains expressing the indicated Hrr25 proteins were starved for glucose for 24 hr and the relative level of each protein was then assessed by Western blotting. (C) Inhibition of the proteasome stabilized the PLS1* variant upon glucose starvation. Strains expressing the indicated Hrr25 proteins were starved for glucose for 24 hr with or without the proteasome inhibitor, MG-132 (100 μM). The relative level of each protein was assessed by Western blotting (left) and quantified with the ImageJ software package (right). (D) A model showing how the localization to P-bodies sequesters Hrr25 away from the degradation machinery in the cytoplasm.

the cytoplasm. Targeting-defective variants of Hrr25 that fail to localize to P-bodies were degraded when cells were exposed to a granule-inducing stress. Thus, the decision to associate with an RNP granule can influence the ultimate fate of the recruited protein. The sequestration in the granule would provide the cell with a pool of active Hrr25 that could be deployed when the initiating stress is removed. This work therefore advances our understanding of the mechanisms controlling protein recruitment to RNP granules and the potential consequences for the localized protein. Determining the broader physiological relevance of this pool of protein is the next step in the analysis and is a primary focus of our

current research efforts. Since we know rather little currently about the biological roles of the P-body, the continuation of this work should further our understanding of these and related RNP granules in the eukaryotic cell.

Acknowledgments

We thank Tien-Hsien Chang, Martha Cyert, Harold Fisk, Anita Hopper, Roy Parker, Daniel Schoenberg, Jeremy Thorner, and Claudio de Virgilio for reagents used in this study; Harold Fisk, Anita Hopper, and Jian-Qiu Wu for access to their equipment; Kevin Corbett for sharing Hrr25 structural data prior to publication; Megan Emerson and Anna Butler for technical support; and members of the Herman lab, especially Regina Nostramo, for helpful discussions and comments on the manuscript. This work was supported by grants GM-101191 and GM-065227 from the National Institutes of Health (to P.K.H.) and a graduate student fellowship from the Pelotonia Fellowship Program (to B.Z.).

Literature Cited

Anderson, P., and N. Kedersha, 2009 RNA granules: post-transcriptional and epigenetic modulators of gene expression. Nat. Rev. Mol. Cell Biol. 10: 430–436.

Anderson, P., N. Kedersha, and P. Ivanov, 2015 Stress granules, P-bodies and cancer. Biochim. Biophys. Acta 1849: 861–870.

Arimoto, K., H. Fukuda, S. Imajoh-Ohmi, H. Saito, and M. Takekawa, 2008 Formation of stress granules inhibits apoptosis by suppressing stress-responsive MAPK pathways. Nat. Cell Biol. 10: 1324–1332.

Ashe, M. P., S. K. De Long, and A. B. Sachs, 2000 Glucose depletion rapidly inhibits translation initiation in yeast. Mol. Biol. Cell 11: 833–848.

Balagopal, V., and R. Parker, 2009 Polysomes, P bodies and stress granules: states and fates of eukaryotic mRNAs. Curr. Opin. Cell Biol. 21: 403–408.

Bashkirov, V. I., H. Scherthan, J. A. Solinger, J. M. Buerstedde, and W. D. Heyer, 1997 A mouse cytoplasmic exoribonuclease (mXRN1p) with preference for G4 tetraplex substrates. J. Cell Biol. 136: 761–773.

Beckham, C. J., H. R. Light, T. A. Nissan, P. Ahlquist, R. Parker *et al.*, 2007 Interactions between brome mosaic virus RNAs and cytoplasmic processing bodies. J. Virol. 81: 9759–9768.

Beelman, C. A., A. Stevens, G. Caponigro, T. E. LaGrandeur, L. Hatfield *et al.*, 1996 An essential component of the decapping enzyme required for normal rates of mRNA turnover. Nature 382: 642–646.

Bishop, A. C., O. Buzko, and K. M. Shokat, 2001 Magic bullets for protein kinases. Trends Cell Biol. 11: 167–172.

Biswas, A., S. Mukherjee, S. Das, D. Shields, C. W. Chow *et al.*, 2011 Opposing action of casein kinase 1 and calcineurin in nucleo-cytoplasmic shuttling of mammalian translation initiation factor eIF6. J. Biol. Chem. 286: 3129–3138.

Brangwynne, C. P., 2011 Soft active aggregates: mechanics, dynamics and self-assembly of liquid-like intracellular protein bodies. Soft Matter 7: 3052–3059.

Brangwynne, C. P., C. R. Eckmann, D. S. Courson, A. Rybarska, C. Hoege *et al.*, 2009 Germline P granules are liquid droplets that localize by controlled dissolution/condensation. Science 324: 1729–1732.

Brangwynne, C. P., T. J. Mitchison, and A. A. Hyman, 2011 Active liquid-like behavior of nucleoli determines their size and shape in Xenopus laevis oocytes. Proc. Natl. Acad. Sci. USA 108: 4334–4339.

Buchan, J. R., J. H. Yoon, and R. Parker, 2011 Stress-specific composition, assembly and kinetics of stress granules in Saccharomyces cerevisiae. J. Cell Sci. 124: 228–239.

Budovskaya, Y. V., H. Hama, D. B. DeWald, and P. K. Herman, 2002 The C terminus of the Vps34p phosphoinositide 3-kinase is necessary and sufficient for the interaction with the Vps15p protein kinase. J. Biol. Chem. 277: 287–294.

Budovskaya, Y. V., J. S. Stephan, F. Reggiori, D. J. Klionsky, and P. K. Herman, 2004 The Ras/cAMP-dependent protein kinase signaling pathway regulates an early step of the autophagy process in Saccharomyces cerevisiae. J. Biol. Chem. 279: 20663–20671.

Cary, G. A., D. B. Vinh, P. May, R. Kuestner, and A. M. Dudley, 2015 Proteomic Analysis of Dhh1 Complexes Reveals a Role for Hsp40 Chaperone Ydj1 in Yeast P-Body Assembly. G3 (Bethesda) 5: 2497–2511.

Cougot, N., S. Babajko, and B. Seraphin, 2004 Cytoplasmic foci are sites of mRNA decay in human cells. J. Cell Biol. 165: 31–40.

Decker, C. J., D. Teixeira, and R. Parker, 2007 Edc3p and a glutamine/asparagine-rich domain of Lsm4p function in processing body assembly in Saccharomyces cerevisiae. J. Cell Biol. 179: 437–449.

DeMaggio, A. J., R. A. Lindberg, T. Hunter, and M. F. Hoekstra, 1992 The budding yeast HRR25 gene product is a casein kinase I isoform. Proc. Natl. Acad. Sci. USA 89: 7008–7012.

Eulalio, A., I. Behm-Ansmant, and E. Izaurralde, 2007a P bodies: at the crossroads of post-transcriptional pathways. Nat. Rev. Mol. Cell Biol. 8: 9–22.

Eulalio, A., I. Behm-Ansmant, D. Schweizer, and E. Izaurralde, 2007b P-body formation is a consequence, not the cause, of RNA-mediated gene silencing. Mol. Cell. Biol. 27: 3970–3981.

Eystathioy, T., A. Jakymiw, E. K. Chan, B. Seraphin, N. Cougot *et al.*, 2003 The GW182 protein colocalizes with mRNA degradation associated proteins hDcp1 and hLSm4 in cytoplasmic GW bodies. RNA 9: 1171–1173.

Franks, T. M., and J. Lykke-Andersen, 2008 The control of mRNA decapping and P-body formation. Mol. Cell 32: 605–615.

Giaever, G., A. M. Chu, L. Ni, C. Connelly, L. Riles *et al.*, 2002 Functional profiling of the *Saccharomyces cerevisiae* genome. Nature 418: 387–391.

Gilks, N., N. Kedersha, M. Ayodele, L. Shen, G. Stoecklin *et al.*, 2004 Stress granule assembly is mediated by prion-like aggregation of TIA-1. Mol. Biol. Cell 15: 5383–5398.

Greenan, G., C. P. Brangwynne, S. Jaensch, J. Gharakhani, F. Julicher *et al.*, 2010 Centrosome size sets mitotic spindle length in Caenorhabditis elegans embryos. Curr. Biol. 20: 353–358.

Grozav, A. G., K. Chikamori, T. Kozuki, D. R. Grabowski, R. M. Bukowski *et al.*, 2009 Casein kinase I delta/epsilon phosphorylates topoisomerase IIalpha at serine-1106 and modulates DNA cleavage activity. Nucleic Acids Res. 37: 382–392.

Herman, P. K., and S. D. Emr, 1990 Characterization of VPS34, a gene required for vacuolar protein sorting and vacuole segregation in Saccharomyces cerevisiae. Mol. Cell. Biol. 10: 6742–6754.

Ho, Y., A. Gruhler, A. Heilbut, G. D. Bader, L. Moore *et al.*, 2002 Systematic identification of protein complexes in Saccharomyces cerevisiae by mass spectrometry. Nature 415: 180–183.

Hoekstra, M. F., R. M. Liskay, A. C. Ou, A. J. DeMaggio, D. G. Burbee *et al.*, 1991 HRR25, a putative protein kinase from budding yeast: association with repair of damaged DNA. Science 253: 1031–1034.

Hyman, A. A., C. A. Weber, and F. Julicher, 2014 Liquid-liquid phase separation in biology. Annu. Rev. Cell Dev. Biol. 30: 39–58.

Ingelfinger, D., D. J. Arndt-Jovin, R. Luhrmann, and T. Achsel, 2002 The human LSm1–7 proteins colocalize with the mRNA-degrading enzymes Dcp1/2 and Xrnl in distinct cytoplasmic foci. RNA 8: 1489–1501.

Isoda, M., K. Sako, K. Suzuki, K. Nishino, N. Nakajo *et al.*, 2011 Dynamic regulation of Emi2 by Emi2-bound Cdk1/Plk1/CK1 and PP2A–B56 in meiotic arrest of Xenopus eggs. Dev. Cell 21: 506–519.

Ito, T., T. Chiba, R. Ozawa, M. Yoshida, M. Hattori *et al.*, 2001 A comprehensive two-hybrid analysis to explore the yeast protein interactome. Proc. Natl. Acad. Sci. USA 98: 4569–4574.

Jonas, S., and E. Izaurralde, 2013 The role of disordered protein regions in the assembly of decapping complexes and RNP granules. Genes Dev. 27: 2628–2641.

Kafadar, K. A., H. Zhu, M. Snyder, and M. S. Cyert, 2003 Negative regulation of calcineurin signaling by Hrr25p, a yeast homolog of casein kinase I. Genes Dev. 17: 2698–2708.

Kato, M., T. W. Han, S. Xie, K. Shi, X. Du *et al.*, 2012 Cell-free formation of RNA granules: low complexity sequence domains form dynamic fibers within hydrogels. Cell 149: 753–767.

Kedersha, N., and P. Anderson, 2007 Mammalian stress granules and processing bodies. Methods Enzymol. 431: 61–81.

Kedersha, N., P. Ivanov, and P. Anderson, 2013 Stress granules and cell signaling: more than just a passing phase? Trends Biochem. Sci. 38: 494–506.

Li, Y. R., O. D. King, J. Shorter, and A. D. Gitler, 2013 Stress granules as crucibles of ALS pathogenesis. J. Cell Biol. 201: 361–372.

Longtine, M. S., A. McKenzie, 3rd, D. J. Demarini, N. G. Shah, A. Wach *et al.*, 1998 Additional modules for versatile and economical PCR-based gene deletion and modification in Saccharomyces cerevisiae. Yeast 14: 953–961.

Lord, C., D. Bhandari, S. Menon, M. Ghassemian, D. Nycz *et al.*, 2011 Sequential interactions with Sec23 control the direction of vesicle traffic. Nature 473: 181–186.

Lusk, C. P., D. D. Waller, T. Makhnevych, A. Dienemann, M. Whiteway *et al.*, 2007 Nup53p is a target of two mitotic kinases, Cdk1p and Hrr25p. Traffic 8: 647–660.

Majumder, S., and H. A. Fisk, 2013 VDAC3 and Mps1 negatively regulate ciliogenesis. Cell Cycle 12: 849–858.

Michelitsch, M. D., and J. S. Weissman, 2000 A census of glutamine/asparagine-rich regions: implications for their conserved function and the prediction of novel prions. Proc. Natl. Acad. Sci. USA 97: 11910–11915.

Mitchell, S. F., S. Jain, M. She, and R. Parker, 2013 Global analysis of yeast mRNPs. Nat. Struct. Mol. Biol. 20: 127–133.

Murakami, A., K. Kimura, and A. Nakano, 1999 The inactive form of a yeast casein kinase I suppresses the secretory defect of the sec12 mutant. Implication of negative regulation by the Hrr25 kinase in the vesicle budding from the endoplasmic reticulum. J. Biol. Chem. 274: 3804–3810.

Parker, R., and U. Sheth, 2007 P bodies and the control of mRNA translation and degradation. Mol. Cell 25: 635–646.

Petronczki, M., J. Matos, S. Mori, J. Gregan, A. Bogdanova *et al.*, 2006 Monopolar attachment of sister kinetochores at meiosis I requires casein kinase 1. Cell 126: 1049–1064.

Pilkington, G. R., and R. Parker, 2008 Pat1 contains distinct functional domains that promote P-body assembly and activation of decapping. Mol. Cell. Biol. 28: 1298–1312.

Ramachandran, V., K. H. Shah, and P. K. Herman, 2011 The cAMP-dependent protein kinase signaling pathway is a key regulator of P body foci formation. Mol. Cell 43: 973–981.

Ray, P., U. Basu, A. Ray, R. Majumdar, H. Deng *et al.*, 2008 The Saccharomyces cerevisiae 60 S ribosome biogenesis factor Tif6p is regulated by Hrr25p-mediated phosphorylation. J. Biol. Chem. 283: 9681–9691.

Reijns, M. A., R. D. Alexander, M. P. Spiller, and J. D. Beggs, 2008 A role for Q/N-rich aggregation-prone regions in P-body localization. J. Cell Sci. 121: 2463–2472.

Schafer, T., B. Maco, E. Petfalski, D. Tollervey, B. Bottcher *et al.*, 2006 Hrr25-dependent phosphorylation state regulates organization of the pre-40S subunit. Nature 441: 651–655.

Segal, S. P., T. Dunckley, and R. Parker, 2006 Sbp1p affects translational repression and decapping in Saccharomyces cerevisiae. Mol. Cell. Biol. 26: 5120–5130.

Shah, K. H., R. Nostramo, B. Zhang, S. N. Varia, B. M. Klett *et al.*, 2014 Protein kinases are associated with multiple, distinct cytoplasmic granules in quiescent yeast cells. Genetics 198: 1495–1512.

She, M., C. J. Decker, N. Chen, S. Tumati, R. Parker *et al.*, 2006 Crystal structure and functional analysis of Dcp2p from Schizosaccharomyces pombe. Nat. Struct. Mol. Biol. 13: 63–70.

Sheth, U., and R. Parker, 2003 Decapping and decay of messenger RNA occur in cytoplasmic processing bodies. Science 300: 805–808.

Simon, E., and D. Kornitzer, 2014 Pulse-chase analysis to measure protein degradation. Methods Enzymol. 536: 65–75.

Stoecklin, G., T. Mayo, and P. Anderson, 2006 ARE-mRNA degradation requires the 5′-3′ decay pathway. EMBO Rep. 7: 72–77.

Takahara, T., and T. Maeda, 2012 Transient sequestration of TORC1 into stress granules during heat stress. Mol. Cell 47: 242–252.

Teixeira, D., and R. Parker, 2007 Analysis of P-body assembly in Saccharomyces cerevisiae. Mol. Biol. Cell 18: 2274–2287.

Thedieck, K., B. Holzwarth, M. T. Prentzell, C. Boehlke, K. Klasener *et al.*, 2013 Inhibition of mTORC1 by astrin and stress granules prevents apoptosis in cancer cells. Cell 154: 859–874.

Thomas, M. G., M. Loschi, M. A. Desbats, and G. L. Boccaccio, 2011 RNA granules: the good, the bad and the ugly. Cell. Signal. 23: 324–334.

van Dijk, E., N. Cougot, S. Meyer, S. Babajko, E. Wahle *et al.*, 2002 Human Dcp2: a catalytically active mRNA decapping enzyme located in specific cytoplasmic structures. EMBO J. 21: 6915–6924.

Varia, S., D. Potabathula, Z. Deng, A. Bubulya, and P. A. Bubulya, 2013 Btf and TRAP150 have distinct roles in regulating subcellular mRNA distribution. Nucleus 4: 229–240.

Wang, N., L. Lo Presti, Y. H. Zhu, M. Kang, Z. Wu *et al.*, 2014 The novel proteins Rng8 and Rng9 regulate the myosin-V Myo51 during fission yeast cytokinesis. J. Cell Biol. 205: 357–375.

Weber, S. C., and C. P. Brangwynne, 2012 Getting RNA and protein in phase. Cell 149: 1188–1191.

Wippich, F., B. Bodenmiller, M. G. Trajkovska, S. Wanka, R. Aebersold *et al.*, 2013 Dual specificity kinase DYRK3 couples stress granule condensation/dissolution to mTORC1 signaling. Cell 152: 791–805.

Communicating editor: D. J. Lew

GENETICS

Supporting Information
www.genetics.org/lookup/suppl/doi:10.1534/genetics.116.187419/-/DC1

The Activity-Dependent Regulation of Protein Kinase Stability by the Localization to P-Bodies

Bo Zhang, Qian Shi, Sapna N. Varia, Siyuan Xing, Bethany M. Klett, Laura A. Cook, and Paul K. Herman

DOI: 10.1534/genetics.116.187419

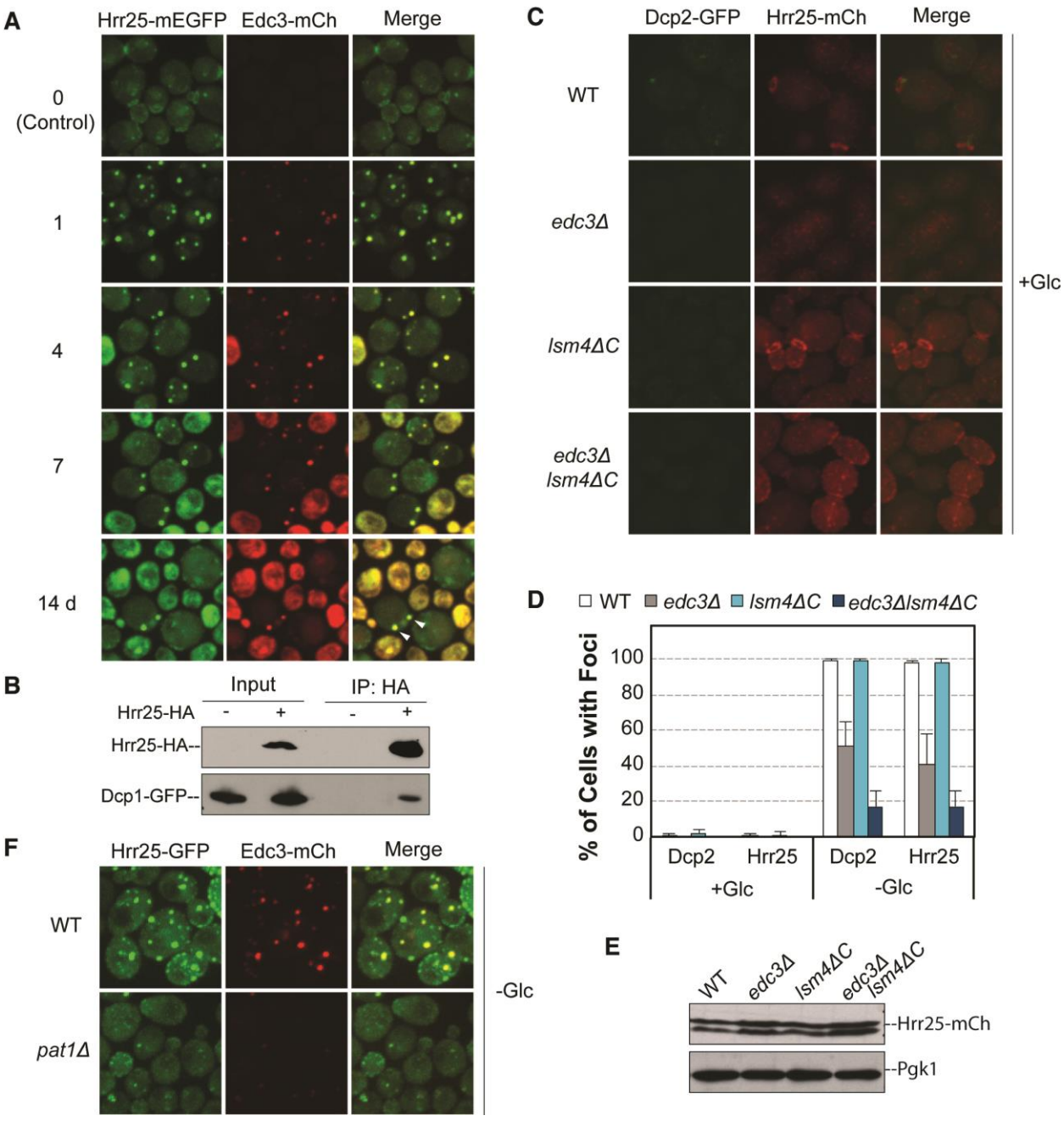

Figure S1 Hrr25 foci formation was dependent upon the presence of P-bodies.

(A) Hrr25 was associated with P-bodies in both the stationary phase and post-diauxic shift growth periods. Yeast cells expressing Hrr25-mEGFP and Edc3-mCh were grown for the indicated number of days in SCD minimal medium and protein localization was examined by confocal microscopy. *0 (Control)*, refers to cells in the mid-log phase of growth. The white arrowheads indicate the P-bodies in the merged image for the 14 day timepoint. (B) Dcp1 was detected in Hrr25 immunoprecipitates. HA-tagged Hrr25 was precipitated from yeast cell extracts and the amount of the associated Dcp1-GFP protein was assessed by western blotting.

(C) The glucose-containing control cultures for Figure 1E. (D) The graph shows the quantitation of the data presented in Figure 1E and S1C. (E) The levels of the Hrr25 protein were similar in the wild-type, *edc3Δ, lsm4ΔC* and *edc3Δ lsm4ΔC* strains. (F) Hrr25 foci were reduced in number and intensity in a *pat1Δ* strain. Wild-type (*WT*) and *pat1Δ* cells were grown to mid-log phase and then starved for glucose to induce P-body formation.

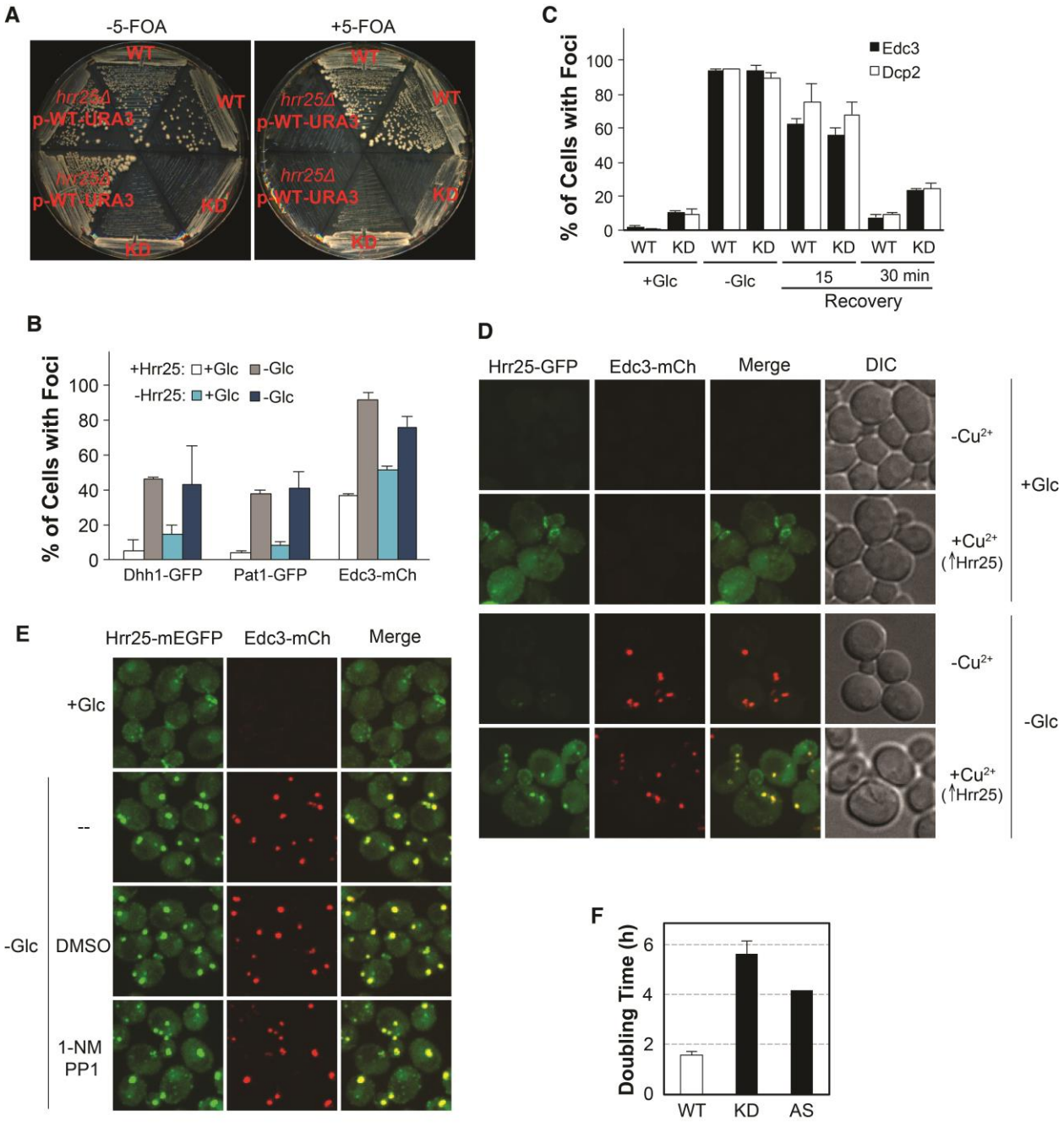

Figure S2 Hrr25 kinase activity was required for its recruitment to P-body foci.

(A) Hrr25 and its kinase activity were required for normal mitotic growth. The indicated strains were plated to minimal medium with or without 5-fluoroorotic acid (*5-FOA*) and incubated at 30˚C for 5 days. The *WT* and *KD* strains expressed a wild-type or kinase-defective version of Hrr25, respectively. To construct the deletion strain, the *HRR25* locus was disrupted in a strain carrying a *URA3* plasmid with the wild type *HRR25* gene. Two isolates of each of the indicated strains were plated; all strains were in the BY4741 genetic background. (B) P-body formation did not require the presence of Hrr25. Cells expressing either the wild-type Hrr25 (*+Hrr25*) or a

Hrr25^{degron} construct that was under the control of a glucose-repressible *GAL* promoter (*-Hrr25*) were grown to mid-log phase in SC minimal medium containing galactose (SCGal) and transferred to SCD medium for 8 hr. The latter incubation resulted in a growth arrest due to the turnover of the degron-tagged Hrr25. The cells were subsequently transferred to SC medium lacking glucose (and galactose) and P-body formation was assessed by fluorescence microscopy. The graphs indicate the fraction of cells with foci for three different P-body reporters. (C) Cells lacking Hrr25 kinase activity did not exhibit a significant defect in P-body disassembly. P-bodies were induced in cells expressing the indicated Hrr25 protein by a transfer to a medium lacking glucose for 30 min (*-Glc*). P-body disassembly was then triggered by the addition of a medium containing 0.2% glucose (*Recovery*). P-body foci were visualized by fluorescence microscopy after 15 or 30 min in the latter medium. (D) P-body formation was not affected by Hrr25 overexpression. P-body formation was assessed in cells containing a plasmid with a *HRR25-GFP* construct under the control of the copper-inducible promoter from the *CUP1* gene. Hrr25-GFP expression was induced by the addition of 100 μM $CuSO_4$ for 2 hr prior to glucose starvation. (E) Treatment with the ATP analog, 1-NM PP1, did not affect the localization of the wild-type Hrr25 protein. (F) Strains expressing the Hrr25^{KD} and Hrr25^{AS} variants exhibited a significantly slower growth rate than wild-type cells. The graph shows the doubling time for strains expressing the indicated Hrr25 proteins in SCD minimal medium at 30°C; the Hrr25^{AS} strain was grown in the presence of the drug, 1-NM PP1.

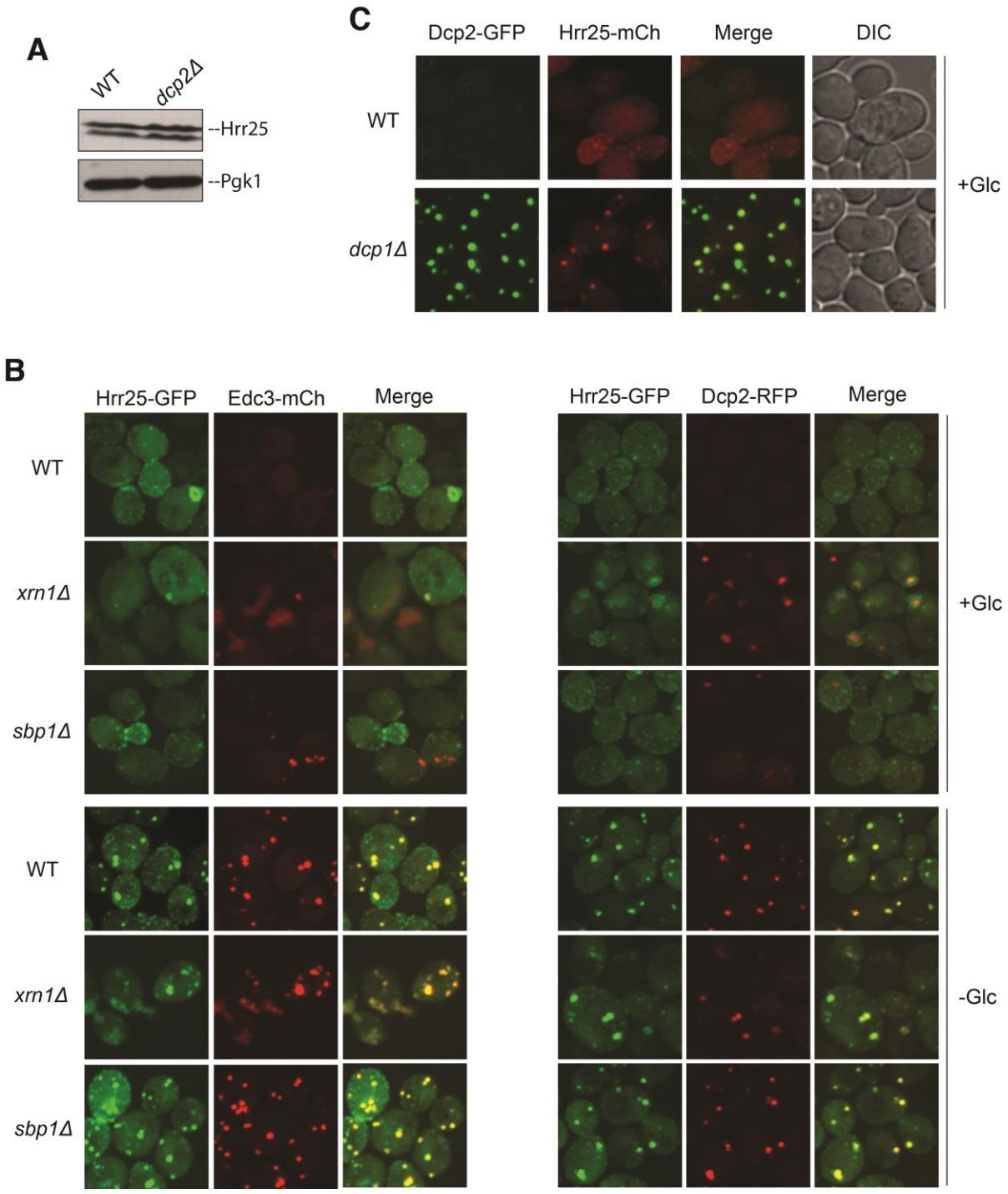

Figure S3 Hrr25 was detected in P-bodies during log phase in *xrn1Δ* mutants.

(A) A western blot showing that Hrr25 expression levels were similar in wild-type and *dcp2Δ* cells. (B, C) The indicated strains were examined by confocal microscopy in mid-log phase (+*Glc*) or after transfer to a medium lacking glucose (-*Glc*). The strains expressed Hrr25 and either Edc3 or Dcp2 tagged with the indicated fluorescent proteins.

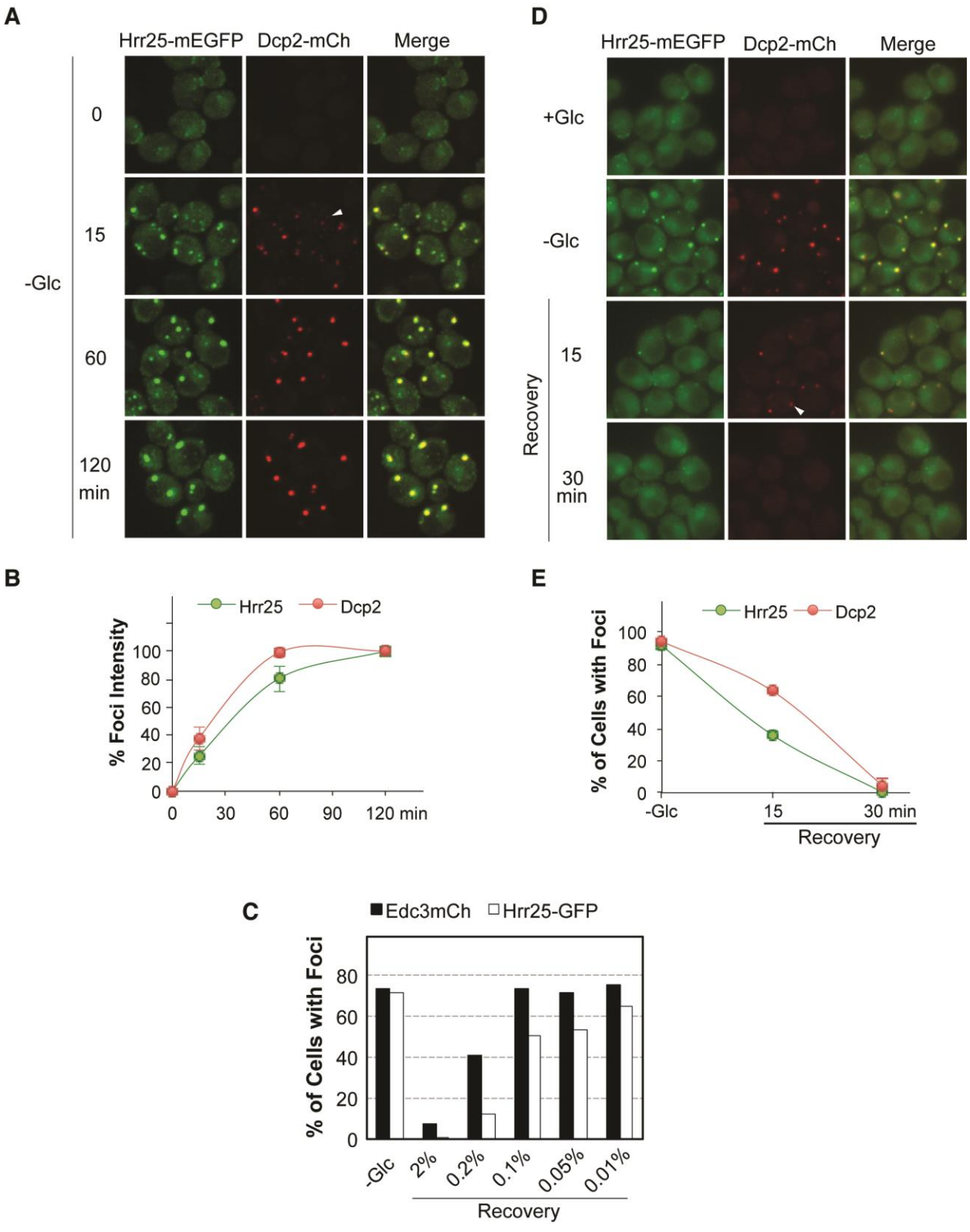

Figure S4 The kinetics of Hrr25 recruitment to, and exit from, P-body foci.

(A, B) Hrr25 was recruited to P-body foci with slower kinetics than Dcp2. Cells expressing Hrr25-mEGFP and Dcp2-mCh were transferred to a medium lacking glucose and visualized by confocal microscopy at the indicated times. The graph in panel *B* indicates the average fluorescence intensities of foci at the indicated times. (C) The effect of glucose concentration on the disassembly kinetics of P-bodies. Cells expressing Hrr25-mEGFP and Edc3-mCh were grown to mid-log phase and then transferred to SC medium lacking glucose to induce P-body formation. The cells were then transferred to media containing the indicated levels of glucose for 15 min and examined by fluorescence microscopy. (D, E) The loss of Hrr25 foci was more rapid than that observed for Dcp2 following glucose re-addition. Cells expressing Hrr25-mEGFP and Dcp2-mCh were transferred from a medium lacking glucose to SC minimal containing 0.2% glucose to induce P-body disassembly (*Recovery*). Cells were visualized by fluorescence microscopy at the indicated times (D) and the percentage of cells with foci were quantified (E). The white arrowheads indicate Dcp2-containing foci with little, if any, Hrr25-associated fluorescence.

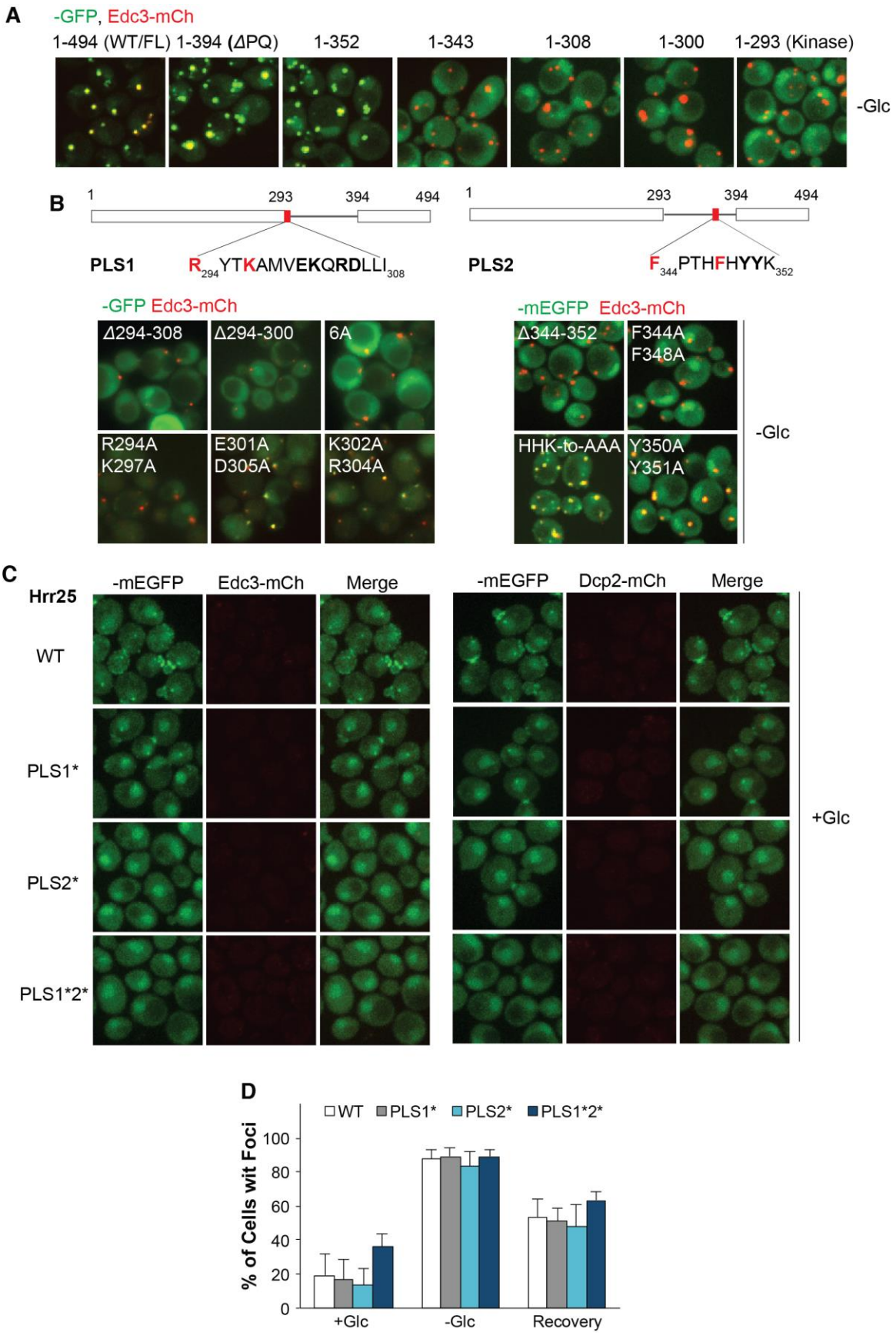
A
-GFP, Edc3-mCh
1-494 (WT/FL)
1-394 (ΔPQ)
1-352
1-343
1-308
1-300
1-293 (Kinase)
-Glc
B
1
293
394
494
PLS1
R294YTKAMVEKQRDLLI308
PLS2
F344PTHFHYYK352
-GFP Edc3-mCh
Δ294-308
Δ294-300
6A
R294A K297A
E301A D305A
K302A R304A
-mEGFP Edc3-mCh
Δ344-352
F344A F348A
HHK-to-AAA
Y350A Y351A
-Glc
C
Hrr25
-mEGFP
Edc3-mCh
Merge
Dcp2-mCh
WT
PLS1*
PLS2*
PLS1*2*
+Glc
D
WT
PLS1*
PLS2*
PLS1*2*
% of Cells wit Foci
0
20
40
60
80
100
+Glc
-Glc
Recovery

Figure S5 The PLS1 and PLS2 elements in the central domain of Hrr25 are required for its efficient localization to P-body foci.

(A) Deletion mapping within the central domain of Hrr25. The intracellular localization of GFP-fusion proteins containing the indicated fragments of Hrr25 was assessed by confocal and fluorescent microscopy. (B) Mutagenesis experiments identified critical residues in the PLS1 and PLS2 localization motifs. The intracellular localization of Hrr25-mEGFP fusion proteins containing the indicated amino acid alterations was assessed by confocal or fluorescence microscopy. Each variant was expressed from the endogenous *HRR25* promoter. (C) The control experiments in glucose-containing medium (+*Glc*) for the data shown in Figure 5C. (D) P-body disassembly was not affected by these central domain mutations. Strains expressing the indicated mEGFP-tagged Hrr25 variants were starved for glucose for 30 min to induce P-body formation (-*Glc*). The cells were then transferred to SC medium containing 0.2% glucose and incubated for 15 min at 30°C. Cells were visualized by fluorescent microscopy and the percentage of cells with foci was quantified.

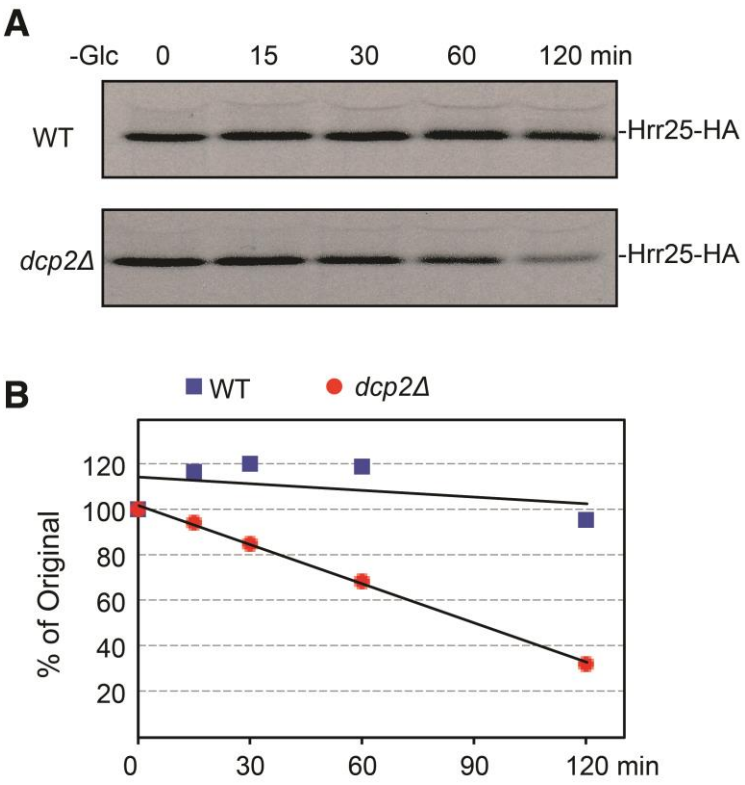

Figure S6 Hrr25 protein turnover occurred at an increased rate in the *dcp2Δ* mutant.

The relative level of the Hrr25 protein was assessed in wild-type and *dcp2Δ* cells as described in the Materials and Methods. Briefly, yeast cells were incubated with the Tran^{35}S-label mixture for 15 mins at 30°C. The labeling reaction was terminated by the addition of a chase solution that resulted in final methionine and cysteine concentrations of 5 mM and 1 mM, respectively. Samples were then collected at the indicated times and the relative level of Hrr25 protein was assessed by autoradiography following immunoprecipitation and SDS-polyacrylamide gel electrophoresis. The autoradiograph and subsequent quantitation of the relative band intensities are shown in panels A and B, respectively.

Table S1 Yeast deletion strains screened for Hrr25 P-body localization.

STANDARD NAME	SYSTEMATIC NAME	STANDARD NAME	SYSTEMATIC NAME
bfr1Δ	YOR198C	*npl3Δ*	YDR432W
bre5Δ	YNR051C	*pby1Δ*	YBR094W
ccr4Δ	YAL021C	*pop2Δ*	YNR052C
*dcp1Δ**	YOL149W	*psp1Δ*	YDR505C
*dcp2Δ**	YNL118C	*psp2Δ*	YML017W
dcs2Δ	YOR173W	*rbp4Δ*	YJL140W
dhh1Δ	YDL160C	*sbp1Δ*	YHL034C
ebs1Δ	YDR206W	*scd6Δ*	YPR129W
ecm32Δ	YER176W	*slf1Δ*	YDR515W
elp1Δ	YLR384C	*slh1Δ*	YGR271W
gbp2Δ	YCL011C	*sro9Δ*	YCL037C
gis2Δ	YNL255C	*tae2Δ*	YPL009C
khd1	YBL032W	*tif4631Δ*	YGR162W
ksp1Δ	YHR082C	*tif4632Δ*	YGL049C
lsm1Δ	YJL124C	*upf1Δ*	YMR080C
lsm6Δ	YDR378C	*upf2Δ*	YHR077C
lsm7Δ	YNL147W	*upf3Δ*	YGR072W
mrn1Δ	YPL184C	*vts1Δ*	YOR359W
nab6Δ	YML117W	*xrn1Δ*	YGL173C
ngr1Δ	YBR212W	*YBR238CΔ*	*YBR238C*
not3Δ	YIL038C	*YGR250CΔ*	*YGR250C*
not4Δ	YER068W		

All strains are from the yeast knockout collection (Open Biosystems) except those marked with an asterisk, the genotype of which are listed in Table S2.

Table S2 Yeast strains used in this study.

STRAIN	GENOTYPE	REFERENCE /SOURCE
PHY5269	*MATa his3Δ1 leu2Δ0 met15Δ0 ura3Δ0* (BY4741)	Invitrogen
PHY4989	*MATa his3Δ1 leu2Δ0 met15Δ0 ura3Δ0 HRR25-GFP:: HIS3MX6*	Invitrogen
PHY6238	*MATa his3Δ1 leu2Δ0 met15Δ0 ura3Δ0 HRR25-mEGFP:: HIS3 EDC3-mCherry::LEU2*	This study
PHY5259	*MATa his3Δ1 leu2Δ0 met15Δ0 ura3Δ0 DHH1-TAP::HIS3MX6*	Open Biosystems
PHY5260	*MATa his3Δ1 leu2Δ0 met15Δ0 ura3Δ0 EDC3-TAP::HIS3MX6*	Open Biosystems
PHY5261	*MATa his3Δ1 leu2Δ0 met15Δ0 ura3Δ0 PAT1-TAP::HIS3MX6*	Open Biosystems
PHY5427	*MATa his3Δ1 leu2Δ0 met15Δ0 ura3Δ0 DCP1-GFP::HIS3MX6*	Invitrogen
PHY4827 (yRP2162)	*MATa leu2-3.112 trp1 ura3-52 his4-539 cup1::LEU2/PGK1pG/MFA2pG DCP2-GFP (NEO)*	(Decker *et al.* 2007)
PHY4828 (yRP2164)	*MATa leu2-3.112 trp1 ura3-52 his4-539 cup1::LEU2/PGK1pG/MFA2pG* ***edc3::NEO*** *DCP2-GFP (NEO)*	(Decker *et al.* 2007)
PHY4829 (yRP2339)	*MATa leu2-3.112 trp1 ura3-52 his4-539 cup1::LEU2/PGK1pG/MFA2pG* ***lsm4 C::NEO*** *DCP2-GFP (NEO)*	(Decker *et al.* 2007)
PHY4830 (yRP2340)	*MATa leu2-3.112 trp1 ura3-52 his4-539 cup1::LEU2/PGK1pG/MFA2pG* ***edc3::NEO lsm4 C::NEO*** *DCP2-GFP (NEO)*	(Decker *et al.* 2007)
PHY4311	*MATα his3 leu2 ura3*	(Coller and Parker 2005)
PHY4313	*MATα his3 leu2 ura3 pat1:: NEO*	(Coller and Parker 2005)
PHY6755	*MATa his3Δ1 leu2Δ0 met15Δ0 ura3Δ0 HRR25-mEGFP:: HIS3 DCP2-mCherry::LEU2*	This study
PHY6265	*MATa his3Δ1 leu2Δ0 met15Δ0 ura3Δ0 HRR25-mEGFP:: HIS3 SPC42-mCherry::LEU2*	This study
PHY5695 (YPH499)	*MATa ura3-52 lys2-801 ade2-101 trp-63 his3-200 leu2-1*	(Kafadar *et al.* 2003)
PHY5675 (KKY387)	*MATa ura3-52 lys2-801 ade2-101 trp-63 his3-200 leu2-1 hrr25::loxP-kanMX-loxP pGAL-3HA-HRR25^{degron}*	(Kafadar *et al.* 2003)
PHY5442	*MATa his3Δ1 leu2Δ0 met15Δ0 ura3Δ0 EDC3-mCherry::Leu2*	This study

PHY7538	*MATa his3Δ1 leu2Δ0 met15Δ0 ura3Δ0 HRR25^{KD}-mEGFP::HIS3 EDC3-mCherry::LEU2*	This study
PHY7539	*MATa his3Δ1 leu2Δ0 met15Δ0 ura3Δ0 HRR25^{KD}-mEGFP::HIS3 DCP2-mCherry::LEU2*	This study
PHY4834 (yRP1724)	*MATa leu2-3.112 trp1 ura3-52 his4-539 cup1::LEU2/PGK1pG/MFA2pG DHH1-GFP (NEO)*	(Sheth and Parker 2003)
PHY4835 (yRP2216)	*MATa leu2-3.112 trp1 ura3-52 his4-539 cup1::LEU2/PGK1pG/MFA2pG **dcp2::TRP1** DHH1-GFP (NEO)*	(Teixeira and Parker 2007)
PHY4832 (yRP1936)	*MATa leu2-3.112 trp1 ura3-52 his4-539 cup1::LEU2/PGK1pG/MFA2pG **dcp1::URA3** DCP2-GFP (NEO)*	(Brengues *et al.* 2005)
PHY4820	*MATa his3Δ1 leu2Δ0 met15Δ0 ura3Δ0 xrn1::KAN*	Open Biosystems
PHY5537	*MATa his3Δ1 leu2Δ0 met15Δ0 ura3Δ0 sbp1::KAN*	Open Biosystems
PHY6873	*MATa his3Δ1 leu2Δ0 met15Δ0 ura3Δ0 HRR25-mEGFP::HIS3 DCP2-TAP::LEU2*	This study
PHY6262	*MATa his3Δ1 leu2Δ0 met15Δ0 ura3Δ0 HRR25^{AS}-mEGFP::HIS3 EDC3-mCherry::LEU2*	This study
PHY6950	*MATa his3Δ1 leu2Δ0 met15Δ0 ura3Δ0 HRR25^{AS}-mEGFP::HIS3 DCP2-TAP::LEU2*	This study
PHY7442	*MATa his3Δ1 leu2Δ0 met15Δ0 ura3Δ0 HRR25^{PLS1*}-mEGFP::HIS3 EDC3-mCherry::LEU2*	This study
PHY7447	*MATa his3Δ1 leu2Δ0 met15Δ0 ura3Δ0 HRR25^{PLS1*}-mEGFP::HIS3 DCP2-mCherry::LEU2*	This study
PHY6249	*MATa his3Δ1 leu2Δ0 met15Δ0 ura3Δ0 HRR25^{PLS2*}-mEGFP::HIS3 EDC3-mCherry::LEU2*	This study
PHY6958	*MATa his3Δ1 leu2Δ0 met15Δ0 ura3Δ0 HRR25^{PLS2*}-mEGFP::HIS3 DCP2-mCherry::LEU2*	This study
PHY7450	*MATa his3Δ1 leu2Δ0 met15Δ0 ura3Δ0 HRR25^{PLS1*2*}-mEGFP::HIS3 EDC3-mCherry::LEU2*	This study
PHY7451	*MATa his3Δ1 leu2Δ0 met15Δ0 ura3Δ0 HRR25^{PLS1*2*}-mEGFP::HIS3 DCP2-mCherry::LEU2*	This study
PHY7541	*MATa his3Δ1 leu2Δ0 met15Δ0 ura3Δ0 HRR25^{PLS1*}-mEGFP::HIS3 DCP2-TAP::LEU2*	This study
PHY6956	*MATa his3Δ1 leu2Δ0 met15Δ0 ura3Δ0 HRR25^{PLS2*}-mEGFP::HIS3 DCP2-TAP::LEU2*	This study
PHY7543	*MATa his3Δ1 leu2Δ0 met15Δ0 ura3Δ0 HRR25^{PLS1*2*}-mEGFP::HIS3 DCP2-TAP::LEU2*	This study
PHY7996	*MATa his3Δ1 leu2Δ0 met15Δ0 ura3Δ0 HRR25-mEGFP::HIS3 pdr5::LEU2*	This study
PHY8000	*MATa his3Δ1 leu2Δ0 met15Δ0 ura3Δ0 HRR25^{PLS1*}-mEGFP::HIS3 pdr5::LEU2*	This study

Table S3 Plasmids used in this study.

PLASMID	DESCRIPTION	REFERENCE/SOURCE
pPHY3926	*pFA6a-LEU2*	This study
pPHY3932	*pFA6a-mCherry-LEU2*	This study
pPHY4174	*pFA6a-TAP-LEU2*	This study
pPHY3714	*DCP2-RFP (CEN, LEU2)*	Dr. Claudio de Virgilio
pPHY3785	*PAT1-mCherry (CEN, URA3)*	(Shah *et al.* 2014)
pPHY3698 (pRP1400)	*LSM1-mCherry (CEN, LEU2)*	(Beckham *et al.* 2007)
pPHY3736	*pRS416-HRR25$_{pro}$-HRR25-GFP-ADH1$_{term}$ (CEN, URA3)*	This study
pPHY3741	*pRS416-HRR25$_{pro}$-HRR25-mCherry-ADH1$_{term}$ (CEN, URA3)*	This study
pPHY3803	*pRS416-HRR25$_{pro}$-HRR25-3XHA-ADH1$_{term}$ (CEN, URA3)*	This study
pPHY2659	*DHH1-GFP (CEN, URA3)*	Dr. Tien-Hsien Chang
pPHY3648	*PAT1-GFP (CEN, URA3)*	(Ramachandran *et al.* 2011)
pPHY3660 (pRP1574)	*EDC3-mCherry (CEN, URA3)*	(Buchan *et al.* 2011)
pPHY3808	*pRS416-CUP1$_{pro}$-HRR25-GFP-ADH1$_{term}$ (CEN, URA3)*	This study
pPHY3734	*pRS415-HRR25$_{pro}$-HRR25-GFP-ADH1$_{term}$ (CEN, LEU2)*	This study
pPHY4231	*pRS414-HRR25$_{pro}$-HRR25-mCherry-ADH1$_{term}$ (CEN, TRP1)*	This study
pPHY4182	*pRS416-GPD$_{pro}$-HRR25^{Central}-GFP-ADH1$_{term}$ (CEN, URA3)*	This study

Supplemental Literature Cited

Beckham, C. J., Light, H. R., Nissan, T. A., Ahlquist, P., Parker, R. *et al.*, 2007 Interactions between brome mosaic virus RNAs and cytoplasmic processing bodies. *J Virol* **81:** 9759-9768.

Brengues, M., Teixeira, D., Parker, R., 2005 Movement of eukaryotic mRNAs between polysomes and cytoplasmic processing bodies. *Science* **310:** 486-489.

Buchan, J. R., Yoon, J. H., Parker, R., 2011 Stress-specific composition, assembly and kinetics of stress granules in Saccharomyces cerevisiae. *J Cell Sci* **124:** 228-239.

Coller, J., Parker, R., 2005 General translational repression by activators of mRNA decapping. *Cell* **122:** 875-886.

Decker, C. J., Teixeira, D., Parker, R., 2007 Edc3p and a glutamine/asparagine-rich domain of Lsm4p function in processing body assembly in Saccharomyces cerevisiae. *J Cell Biol* **179:** 437-449.

Kafadar, K. A., Zhu, H., Snyder, M., Cyert, M. S., 2003 Negative regulation of calcineurin signaling by Hrr25p, a yeast homolog of casein kinase I. *Genes Dev* **17:** 2698-2708.

Ramachandran, V., Shah, K. H., Herman, P. K., 2011 The cAMP-dependent protein kinase signaling pathway is a key regulator of P body foci formation. *Mol Cell* **43:** 973-981.

Shah, K. H., Nostramo, R., Zhang, B., Varia, S. N., Klett, B. M. *et al.*, 2014 Protein kinases are associated with multiple, distinct cytoplasmic granules in quiescent yeast cells. *Genetics* **198:** 1495-1512.

Sheth, U., Parker, R., 2003 Decapping and decay of messenger RNA occur in cytoplasmic processing bodies. *Science* **300:** 805-808.

Teixeira, D., Parker, R., 2007 Analysis of P-body assembly in Saccharomyces cerevisiae. *Mol Biol Cell* **18:** 2274-2287.